ELSEVIER

Marine Micropaleontology 43 (2001) 239–260

MARINE MICROPALEONTOLOGY

www.elsevier.com/locate/marmicro

Patterns of biotic change in Middle Jurassic to Early Cretaceous Tethyan radiolaria

Taniel Danelian[a,*], Kenneth G. Johnson[b]

[a]*Laboratoire de Micropaléontologie, Université Pierre-et-Marie-Curie (PARIS 6), CNRS FRE 2400, C.104, T.15-25, E4, 4 place Jussieu, 75252 Paris Cedex 05, France*

[b]*Geosciences Research Division, Scripps Institution of Oceanography, University of California, La Jolla, San Diego, CA 92093-0244, USA*

Received 9 October 2000; revised 18 April 2001; accepted 8 May 2001

Abstract

The rate of taxic turnover of nearly 400 radiolarian species/subspecies is analyzed in order to document long term biotic change of plankton during the Middle Jurassic to Early Cretaceous (Aalenian to Aptian). The pattern and dynamic of diversity change is described using four indices: rate of species first and last occurrence, rate of diversification and rate of turnover. Plots of cumulative sampling effort suggest that the analyzed data represent an adequate sample of total standing diversity for most examined stages. Rates of species first occurrence exceed rates of last occurrence for most of the Middle Jurassic, except for the middle Bajocian. In contrast, the Late Jurassic was a time of decreasing radiolarian diversity and the Kimmeridgian records the lowest rate of diversification. It is followed by a dramatic increase in first occurrences near the Jurassic–Cretaceous boundary with as a result the highest rate of diversification recorded in the late Tithonian. Regional radiolarian diversity was stable throughout most of the Early Cretaceous. A stratigraphic permutation test was performed to assess the influence of uneven sampling on the observed pattern of taxic turnover and identified the intervals for which randomly obtained patterns are significantly different from the observed pattern. The Kimmeridgian and late Tithonian events coincide with substantial climate-derived perturbations in water cycling, nutrient supply and oceanic productivity. They point to a negative relationship between radiolarian macroevolution and changes in the state of nutrient availability, although further work is needed to refine the temporal resolution of this relationship and to explore ecological aspects of its causal link with respect to radiolarian evolution.

Keywords: radiolaria; evolution; species-diversity; Jurassic; Cretaceous; Tethys

1. Introduction

Documenting long-term patterns of taxic turnover is a necessary prerequisite to determining the role of changing global environments in shaping the tempo and mode of macroevolution. Here, we present a study of the pattern of diversity change in Mesozoic Radiolaria with the goal of determining the response of plankton to well-documented climatic and oceanographic changes during the Jurassic and Cretaceous. Radiolaria are a major plankton group in the modern oceans and because their fossil remains are known since the Cambrian, the group is the main available proxy to gauge zooplankton health and diversity changes for most of the Phanerozoic. Although the extent to which this is related to phytoplankton

* Corresponding author. Fax: +33-1-44-27-38-31.

E-mail addresses: danelian@ccr.jussieu.fr (T. Danelian), kenjohnson@ucsd.edu (K.G. Johnson).

0377-8398/01/$ - see front matter
PII: S0377-8398(01)00029-9

evolution remains to be explored, particularities in radiolarian ecological and food preferences have the potential to provide valuable insights into the evolution of the regional pelagic ecosystem over timescales of millions to tens of millions of years (Lazarus, 1998; Racki, 1999).

Previous studies on the pattern of radiolarian faunal changes focused on particular time intervals, which are either characterized by well-established mass extinctions (e.g. the P–Tr, Tr–J and K–T boundaries; Yao and Kuwahara, 1997; Carter, 1994; Hollis, 1996; respectively) or punctuated by oceanic anoxic events (e.g. the early Toarcian, Hori, 1997; the mid Cretaceous, Lambert and De Wever, 1996; Erbacher and Thurow, 1997). Other workers based their analysis exclusively on changes in species diversity (Vishnevskaya, 1997). However, for a palaeobiological event to be fully understood, it needs to be analyzed within the framework of the group's evolutionary dynamics, including the relative changes of both origination and extinction rates (Foote, 2000). Moreover, as already pointed out by Roth (1987), the taxic evolution of a group is more completely and accurately described through the direct study of origination and extinction rates, rather than by the simple analysis of patterns in diversity changes.

Some workers have limited their analyses to stratigraphic ranges of higher level taxa, and are wary of using low level data to address global macroevolutionary questions (Sepkoski, 1982). But numerous efforts have focused on species level compilations (Hoffman and Kitchell, 1984; Wei and Kennett, 1986; Roth, 1987; Budd et al., 1996; Johnson et al., 1995; Budd and Johnson, 1999; Johnson and Curry, in press). Analyses of species-level compilations may be more prone to generate sampling and taxonomic artefacts, but new analytical approaches can be used to explore the effect of uneven sampling on the resulting pattern. The confidence interval approach of Marshall (1990, 1994) uses the pattern of occurrences within taxon ranges to estimate confidence regions for the true duration of taxa. These regions represent extensions of the observed range within which the true appearance and disappearance of a taxon can be localized with a stated level of confidence. The result is interpretations that can be judged on the strength of the supporting evidence. Other methods use the stratigraphic distribution of samples and the co-occurrence of taxa to generate permutation distributions against which observed patterns can be compared (Johnson and McCormick, 1999; Budd and Johnson, 2001). In contrast, the probabilistic analyses of Foote and Raup (1996) use only the distribution of stratigraphic ranges of taxa to obtain a total estimate of average sampling completeness for a set of subintervals. Fewer analytical tools are available to test for spurious patterns generated through taxonomic practice. Such artefacts might be caused by uneven distribution of research effort among taxonomic groups and stratigraphic intervals (Signor, 1978), and can be minimized by taking advantage of new compilations of species distributions within a consistent taxonomic framework.

We present here the results of our investigation on the taxic evolution and evolutionary dynamics in Middle Jurassic to Early Cretaceous Tethyan radiolaria. More particularly, we have attempted to estimate rates of taxic turnover and the timing and intensity of changes in taxic turnover during the studied time interval (~60 Ma). We have further attempted to test our dataset with respect to possible effects of sampling bias on the observed patterns. We finally investigate the temporal relationship between the pattern of radiolarian taxic evolution and palaeoceanographic events and discuss the possible driving forces for the evolution of Jurassic and Cretaceous Tethyan radiolaria.

2. Data and methods

2.1. Occurrence data

A recently published Tethyan radiolarian atlas and biozonation (Baumgartner et al., 1995a) provides a substantial amount of biostratigraphic information, based on which the taxic evolution of Middle Jurassic to Lower Cretaceous radiolaria can be explored in a consistent taxonomic framework. This work was compiled by the Jurassic–Cretaceous Working Group of the International Association of Radiolarian Palaeontologists (INTERRAD), following three annual meetings (January 1989, February 1990, March 1991) during which a taxonomic consensus was obtained for over 450 radiolarian species/subspecies. The stratigraphic distribution of taxa was subsequently described from a large number of samples

recovered from numerous Tethyan sections. A new radiolarian biozonation was ultimately constructed following the concepts of Unitary Associations (UA, Guex, 1991), representing maximal sets of mutually co-existing species/subspecies. In practice, each UA is characterized by associations of species/subspecies first and last occurrences. The degree of reproducibility of one or more UA grouped together allows the recognition of biozones (Unitary Association Zones or UAZ). Only the latter (and not the individual Unitary Associations) bear a chronostratigraphic significance.

The UA methodology for constructing a biozonation is particularly well-suited for the patchily preserved radiolarian record and provides assemblages which are linked to each other in an orderly way through time. Moreover, it provides biostratigraphic information for a large number of taxa, which can be used subsequently for the study of radiolarian taxic evolution. However, there are also a number of limitations which need to be explicitly discussed. (1) By the very way of constructing an UA biozonation no evaluation can be made with respect to possible sampling biases on the observed patterns of taxic evolution. This was a particular point which we wished to explore in our analysis (see further below). (2) Stratigraphic details are often sacrificed in order to overcome incompatibilities of the original biostratigraphic dataset. Taking the above Baumgartner et al. (1995b) biozonation for example, composite sections were constructed because the initial dataset contained too many conflicting superpositional relationships between samples. The end product of a 'snowball' procedure was regarded as reflecting 'reasonably well the stratigraphic relationships within the Atlantic–Mediterranean Tethys' (Baumgartner et al., 1995b, p. 1021). (3) There are a number of taxonomic repetitions in the list of taxa analyzed in this biozonation. Some widely defined morphospecies used in the biozonation are split into a number of subspecies, which are also included in the biozonation; for example, *Emiluvia orea* Baumgartner s.l. (sensu Baumgartner et al., 1995c,), includes two subspecies: *E. orea orea* Baumgartner in Baumgartner et al. (1980) and *E. orea ultima* Baumgartner and Dumitrica in Baumgartner et al. (1995c). This was done for practical reasons: if a specialist cannot assign a specimen to one of the subspecies but can assign it to the more widely defined species, this process leads to gain of information. (4) Finally, each new UA biozonation needs to be seen as a step forward in the process of better exploring the stratigraphic record. As new data are accumulated the number of incompatibilities existing within the published biozonation increases. Species which should not co-occur according to the published UA biozonation may be found actually co-occuring in new research material. This has been indeed the case with a number of samples examined by the senior author since the publication of the 1995 biozonation. The only remedy to this problem is to re-calculate the whole set of data, by including the newly found uncompatible co-occurrences (J. Guex, personal communication).

For the above reasons, and in order to examine the possible effects of sampling bias on the pattern of radiolarian taxic evolution we followed a different approach in this study. We compiled a new dataset based on selected data originating from a number of publications included in the volume edited by Baumgartner et al. (1995a; see Appendix A). This new database contains over 7500 radiolarian occurrences of 393 species/subspecies in 198 samples. All selected samples used in our compilation are independently calibrated either by age diagnostic fossils other than radiolaria (i.e. ammonites, calcareous nannofossils, calpionellids) or by isotope and magnetostratigraphy. We thus excluded all samples which are only dated by means of radiolaria in order to avoid circular reasoning (i.e. looking at radiolarian extinctions by using samples dated by radiolaria). Palaeogeographic reconstructions place the selected samples in the central (proto-) Atlantic and Western Tethyan oceans (Fig. 1). We wished to look at a database representing faunal changes recorded in one well-constrained palaeogeographic area. For this reason we excluded data coming from outside the western Tethys–central Atlantic, such as those from British Columbia (Carter, 1995) and the western Pacific (Matsuoka, 1995), which would have otherwise been of much interest. We also excluded widely defined morphospecies (i.e. *E. orea* s.l.) used in the biozonation by Baumgartner et al. (1995b) and retained only the biostratigraphic data of the subspecies to which they are split. The Mesozoic time scale by Gradstein et al. (1995) with the Jurassic modifications by Pálfy et al. (2000) were used to

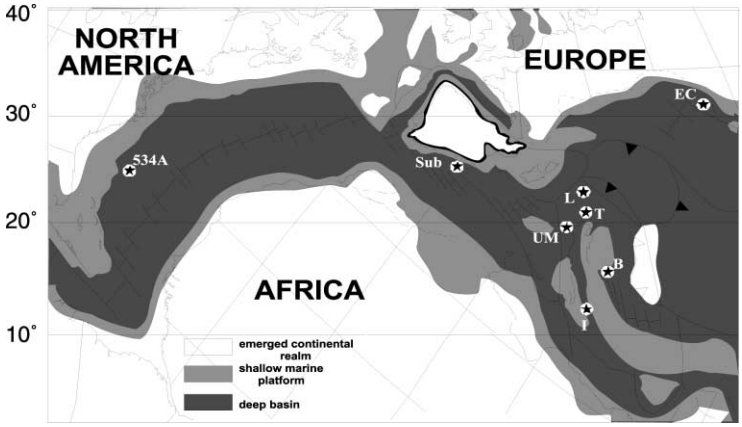

Fig. 1. Late Jurassic (early Tithonian) palaeogeographic position of analyzed sedimentary sections in Western Tethys and Central Northern Atlantic. Palaeogeographic map redrawn after Thierry et al. (2000). 534A = DSDP Site 534A; Sub = Subbetic Realm; EC = Eastern Carpathians; L = Lombardy Basin; T = Trento Plateau; UM = Umbria–Marche, B = Budva Trough; I = Ionian zone.

translate chronostratigraphic intervals into absolute ages. The stratigraphic distribution of the included samples is shown in Fig. 2a. Data are available from the authors or on the world wide web at http://cayo-agua.ucsd.edu/datasets/rads/index.html.

2.2. Stratigraphic ranges and evolutionary rates

The stratigraphic range of each species/subspecies (Fig. 2b and c) was estimated as the time interval extending from the lower age limit of the sample of first occurrence to the upper age boundary of the sample of last occurrence ('long' ranges of Johnson and McCormick, 1999). This approach is likely to be more conservative than midpoint ranges (using only the median age of each sample), because incomplete sampling will always result in underestimates of true species durations. The first and last occurrences for each species/subspecies were found by examining all occurrences for the taxon in consideration. We are aware that it is unlikely that all species first and last occurrences in our dataset represent cladogenetic events and true global extinctions. Most of them might simply be the result of arbitrary subdivisions of evolving lineages, due to the typological taxonomy largely in use for Mesozoic radiolaria. However, there is no stable phylogenetic scheme yet available for Mesozoic radiolaria, and indeed only for very few radiolarian species have phylogenetic relationships been suggested so far (for some examples see Pessango and Blome, 1980; Matsuoka, 1983; Dumitrica and Dumitrica-Jud, 1995; Baumgartner and Bartolini, 1997). Also, some of the faunal turnover observed in the analyzed dataset might be due to exchange with other parts of the Mesozoic oceans situated outside western Tethys and Central North Atlantic. Although the extent of these events are not well known in the plankton, some of the first occurrences in our dataset might be simply due to migrations into the examined biogeographic area, as opposed to true speciation events, and some of the last occurrences might be simply restricted local extinctions, rather than global extinctions. Therefore, we will refrain from using the terms origination and extinction in this contribution. On the other hand, the diversity sampled by using morphologically defined species/subspecies may be underestimating real biological (genetic) diversity which was either not expressed (i.e. cryptic) or very subtly expressed on the preservable characters of fossilized skeletons (see Norris, 2000 for a review). In spite of all the above limitations we believe that given the current state of radiolarian taxonomy, our approach to describe the pace and mode of faunal changes at a regional scale is particularly useful as a proxy to explore the major pattern of evolutionary changes in Mesozoic radiolaria.

To describe the changing pattern of taxic diversity through time we divided the entire study interval into a set of subintervals and calculated species richness

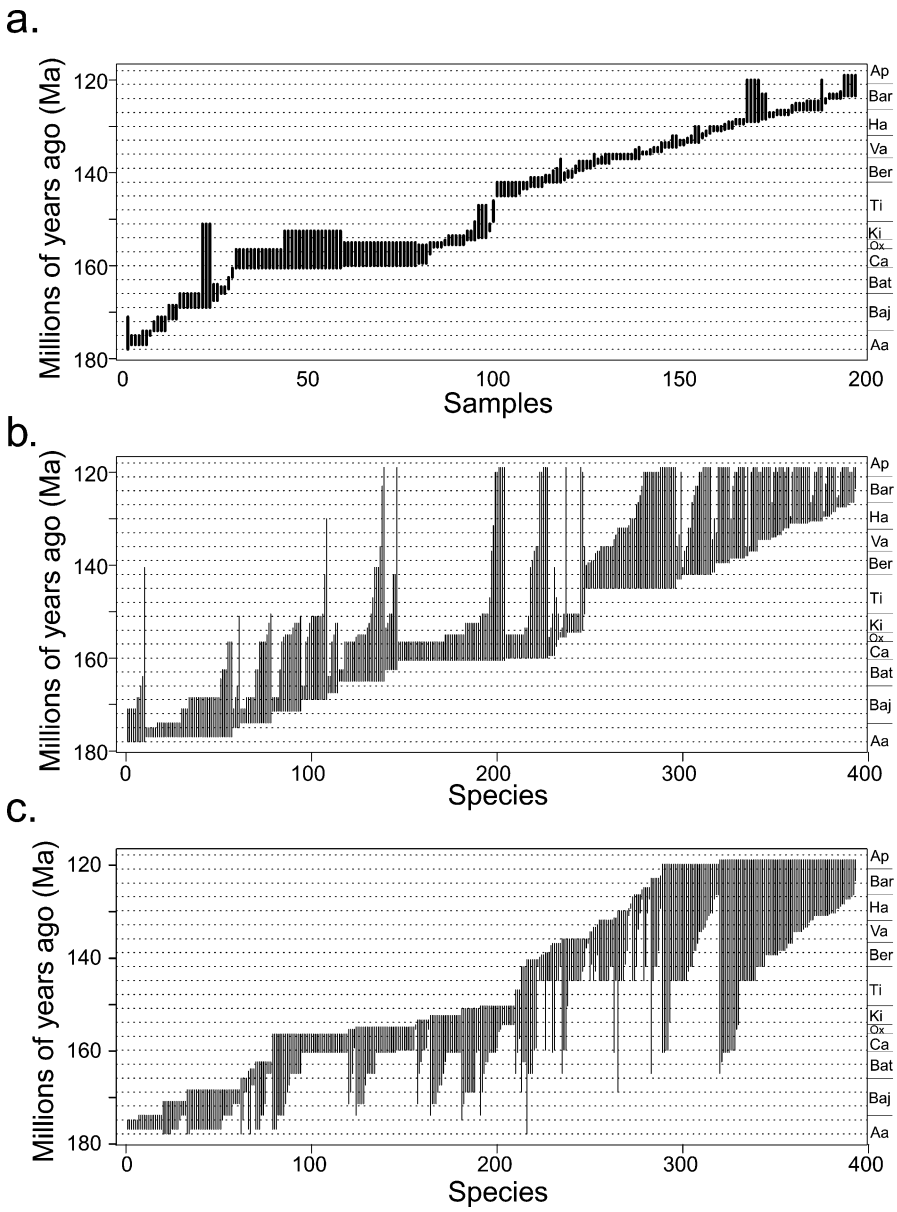

Fig. 2. Stratigraphic ranges of samples (a) and radiolarian species/subspecies (b, c) obtained from analysis of the established Middle Jurassic to Lower Cretaceous distribution database. The median age resolution of samples is 2.75 my, and the mean age resolution is 3.48 my. Species are sorted both by first occurrence (b) and last occurrence (c). The median species range is 10 my, and mean species range is 12.59 my. The horizontal lines indicate three-million year subintervals used in the analysis of taxic turnover. Chronostratigraphy after Pálfy et al. (2000) for the Jurassic and Gradstein et al. (1995) for the Cretaceous. Abbreviations are as follows: Aa = Aalenian, Baj = Bajocian, Bat = Bathonian, Ca = Callovian, Ox = Oxfordian, Ki = Kimmeridgian, Ti = Tithonian, Ber = Berriasian, Va = Valanginian, Ha = Hauterivian, Bar = Barremian, Ap = Aptian.

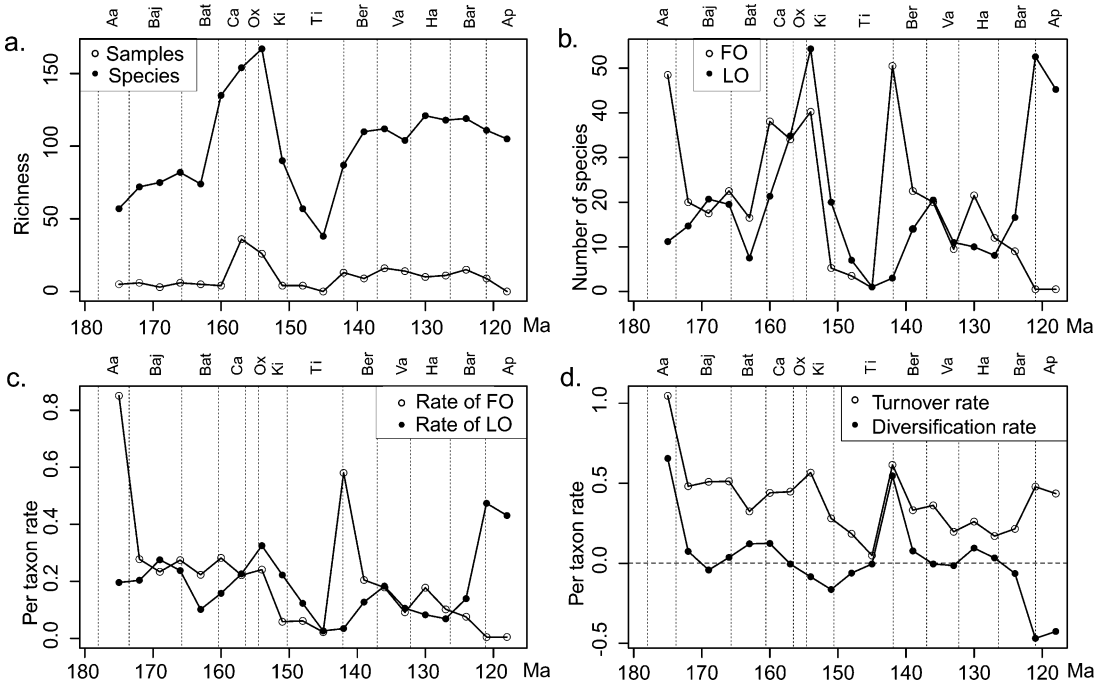

Fig. 3. Plots of the pattern of taxic turnover within the Middle Jurassic to Early Cretaceous radiolaria. Each point indicates results for one three-million year subinterval, with points positioned at the end of the subinterval (i.e. the point shown at 169 Ma corresponds to the subinterval 172–169 Ma). (a) The numbers of samples and species recovered from each subinterval. (b) Numbers of species first (FO) and last (LO) occurrences. (c) Per-taxon rates of first and last occurrence. (d) Rates of taxic diversification and turnover. In each plot the vertical dashed lines indicate the duration of stratigraphic stages (abbreviations as in Fig. 2) following the timescale of Pálfy et al. (2000) for the Jurassic and Gradstein et al. (1995) for the Cretaceous.

and the number of species first and last occurrences within each interval. Selection of subintervals requires a compromise between maximizing the chance of discovering real pattern and accounting for the level of stratigraphic resolution within the data (Johnson and McCormick, 1999). If intervals are too narrow, we might risk interpreting spurious patterns caused by the uneven distribution of samples. But if subintervals are too wide we might miss significant episodes of taxic change within restricted stratigraphic intervals. However, our use of 'long' species ranges and our approach to measuring the taxonomic richness and rates of species first and last occurrence are largely insensitive to bin length. Therefore, we have estimated patterns of change within a set of equal subintervals of three-million year (my) duration that span the stratigraphic interval from 181 to 109 Ma. The 3 my duration represents a compromise given the large age range of some samples in the dataset. The median age resolution of samples is 2.75 my and the mean age resolution is 3.48 my (Fig. 2a). Parallel analyses were performed for alternate stratigraphic subdivisions including coarser and more refined bins. The results were not significantly different than those obtained using three my subintervals and are therefore not presented here.

Species richness was estimated within each subinterval using the range-through method (Johnson and McCormick, 1999) in which total richness is increased by species with stratigraphic ranges that cross any part of the subinterval (Fig. 3a). Use of the range-through method de-emphasizes the importance of alternate schemes for subdividing the study interval, because species will be considered present in subintervals from which they might not actually been recovered. Total richness estimates were used, in which richness is estimated as the total number of species with ranges that cross each stratigraphic bin (Foote, 1994).

Estimates of turnover intensity were obtained

by counting the number of first and last occurrences in each subinterval weighted by the stratigraphic resolution of the sample in which each taxon first or last occurs (Fig. 3b). This approach reduces the likelihood of producing spurious peaks of taxic change due to the combination of narrow stratigraphic bins and poor age resolution (Budd et al., 1996; Budd and Johnson, 1999; Johnson and McCormick, 1999). In the current dataset only 82 of the 196 samples (42%) have sufficient age resolution to be assigned to a single three-million year time interval. Assigned age resolutions of an additional 70 samples (36%) cross two time intervals, and the remaining samples cross three or more intervals. If a taxon first or last occurs in a sample which spans more than one interval, it is impossible to credit a single interval with the first or last occurrence event. One approach would be to assign each first or last occurrence event to the interval containing the midpoint of the key sample. However, this might result in spurious turnover peaks when in fact the species first and last occurrence events were spread throughout a much longer period. Therefore, we have weighted each first or last occurrence event by the length of the key samples in which the event was recognized. If a species first occurs in a sample with an assigned age that falls entirely within a single stratigraphic bin, then that bin is credited with one first occurrence event. However, if a species first occurs in a sample spanning two time intervals, then each of those two intervals will be credited with one half of an origination event. In more general terms, samples that span n stratigraphic bins will contribute $1/n$ first or last occurrences to each bin crossed for each species that first or last occur in the sample (see Fig. 7.3 in Johnson and McCormick, 1999).

We expect to find edge effects in the observed pattern of taxic turnover because we have not sampled beyond the boundaries of a finite stratigraphic interval (Aalenian to early Aptian). Therefore, depending on how well our data represent the fauna, species that are known to occur after the early Aptian will appear to last occur in the upper part of the study interval. For example, the species *Acaeniotyle diaphorogona* Foreman, (1973) (sensu Baumgartner, 1984 and Baumgartner et al., 1995c) is known to occur in the middle Albian of section Apechiese from Umbria–Marche (O'Dogherty, 1994). Therefore the last occurrence of species *A. diaphorogona* within samples GC_882.40, GC_887.00, GC_889.30 and GC_893.30 from the late Barremian–earliest Aptian part of section Gorgo-a-Cerbara (Umbria–Marche, Italy, Dumitrica-Jud, 1995) in our data is incorrect. Additional range truncations will result in a spurious peak of first occurrence near the beginning of the study interval and a similar effect will result in an overestimation of the true number of species last occurrences near the end of the study interval.

A stratigraphic permutation test (Fig. 4) was performed to determine the effects of range truncation near the boundaries of the study interval (Johnson and McCormick, 1999; Budd and Johnson, 1999; Jackson and Johnson, 2000). The test is performed by comparing the observed turnover pattern with a test distribution derived from a large set of randomized patterns generated under the null hypothesis that all observed faunal change is a result of sampling error. Because each sample is characterized by a stratigraphic position and a radiolarian assemblage, randomized data sets could be generated by shuffling the assemblages among samples while keeping the chronostratigraphic position of each sample constant. Therefore both the stratigraphic pattern of sampling and the pattern of species abundance and co-occurrence remains constant, but in each permutation different assemblages are assigned to each sample. Estimates of richness and the numbers of first and last species occurrences per three-million year interval were then calculated using the randomized data to compile a test distribution that included patterns from 1000 randomized data sets. The observed pattern of taxic turnover was compared with the test distribution. If range truncation or uneven sampling results in an artificial peak in the observed pattern of turnover, then this same peak should be found even after the assemblages have been randomly reassigned to samples. Sampling bias cannot be excluded if the observed pattern does not differ significantly from the majority of randomized patterns. We have plotted the 10th and 90th percentiles of the permutation distribution along with observed patterns in Fig. 4. If the observed pattern lies outside of this region then it represents significant pattern. Therefore, large number of first occurrences at the beginning of the dataset (i.e. older than 151 Ma) and of last occurrences at the end of the dataset (younger than 145 Ma), could be artefacts created

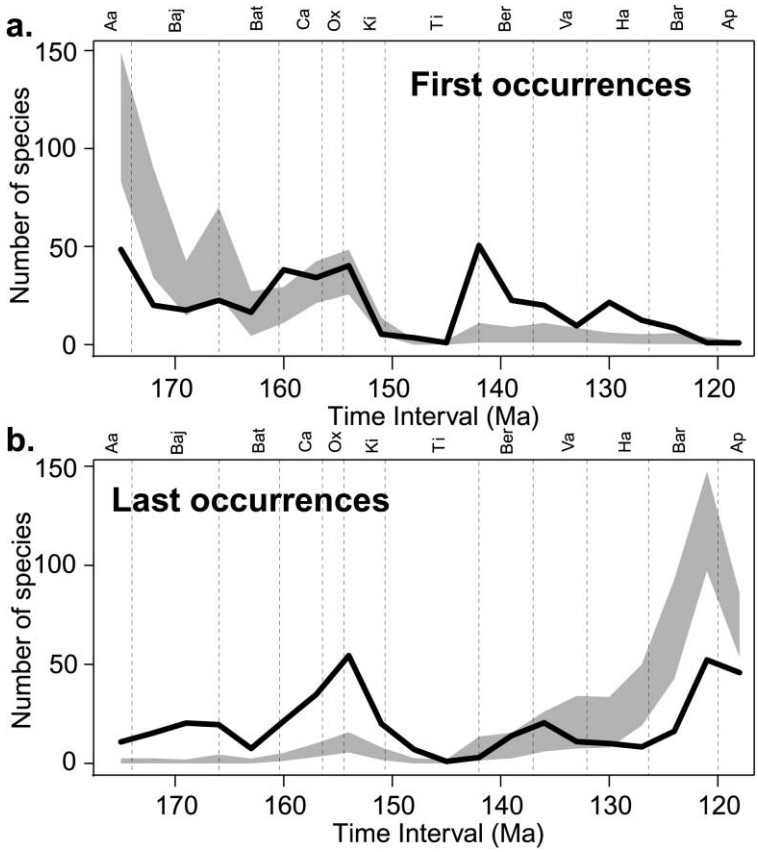

Fig. 4. Results of a stratigraphic permutation test comparing observed number of first (a) and last (b) occurrences with a permutation distribution. On each plot, the black line illustrates the observed pattern, while upper and lower boundaries of the shaded area represent the 10th and 90th percentile of a permutation distribution generated by randomly shuffling assemblages among samples over 1000 iterations. Chronostratigraphy and stratigraphic stage abbreviations as in Fig. 2.

by range truncation outside of the window of sampling. In contrast, those parts of the observed pattern, which are different from a large proportion of randomized patterns are likely to reflect true evolutionary patterns. For example, this is the case for the pattern of species first occurrences discovered in the late Kimmeridgian to Barremian interval, as well as the pattern of last occurrences obtained for the Jurassic intervals (older than 145 Ma).

Both raw counts of the numbers of first and last occurrences and per-taxon rates of turnover intensity were examined, because no single set of estimators are unbiased with respect to standing diversity and subinterval duration (Foote, 1994). Some of the well-known techniques for calculating taxic evolution were used, as these were first described by Simpson (1953) and further explained by Sepkoski (1978), Hoffman and Kitchell (1984) and Roth (1987). Four indices were calculated as summarized below:

Rate of species first occurrence $R_{FO} = (1/D)(FO/\Delta t)$ and the rate of last occurrence $R_{LO} = (1/D)(LO/\Delta t)$,

where D is the total species richness within a subinterval Δt, FO and LO, the number of first and last occurrences in the same subinterval Δt (Fig. 3c).

Because the subinterval length is constant in all analyses presented here, per-taxon rates have not been divided by interval duration. The rate of diversification (Rd) is given by the difference between the rate of first occurrence and that of last occurrence ($Rd = R_{FO} - R_{LO}$), while the rate of turnover is obtained by adding them ($Rt = R_{FO} + R_{LO}$) (Fig. 3d).

2.3. Adequacy of the record

Taphonomic effects could alter the abundance and diversity of siliceous microfossils. Dissolution of siliceous skeletons is a common phenomenon in the modern oceans because they are undersaturated with respect to silica (Lisitzin, 1985). As a result, part of the radiolarian diversity in the plankton is lost in the water-column, although in the Recent there is a close correspondence between diversity of radiolarians in the plankton and those preserved in surface sediments (Renz, 1976). Moreover, the preservation of silica is enhanced under eutrophic water masses, where rich faunas are likely to be recovered (see De Wever et al., 1994 for a review). However, an exclusively actualistic approach may not be entirely justified because the oceans were probably much less silica-starved before the Tertiary emergence of diatoms as major silica producers (Racki and Cordey, 2000).

Variation in the abundance and diversity of radiolarians in the sedimentary record might also be caused by the differential preservation and recovery of fossils from different lithologies. Siliceous radiolaria are more readily extracted from limestones, so are considered to represent a more reliable record than radiolaria extracted from cherts or siliceous mudstones (Hull, 1995; Mekik, 2000). This is partly due to the differential destructive effect of various extraction techniques. For example, hydrofluoric acid (HF) processing of cherts and siliceous mudstones is more harmful to delicate well preserved radiolaria than hydrochloric or acetic acid, biasing thus the fossil assemblage in favor of robust morphotypes (Blome and Reed, 1993). The majority of samples included in the analyzed database (Appendix 1) are siliceous limestones from which radiolaria were extracted with the use of hydrochloric acid, often applied locally to areas surrounding chert nodules or lenses (see Jud 1994 for further details). As the majority of radiolarian assemblages were extracted from similar lithologies and without the use of any very aggressive acids (i.e. HF), we believe that the influence of lithology-linked preservation is homogeneous throughout our data set.

The fossil record is notoriously incomplete and patchily preserved, so some data sets are clearly inappropriate to test large-scale environmental or biological explanations for patterns of biotic change (e.g. Paul, 1982; Donovan and Paul, 1998). Estimates of magnitude and temporal pattern of species richness can be biased by the temporal pattern of sampling completeness, or the proportion of species which are preserved and have been collected (e.g. Raup, 1976; Signor, 1978). Furthermore, variation in sampling completeness among stratigraphic intervals is likely to create spurious patterns in estimates of taxic turnover (Signor and Lipps, 1982; Koch, 1987; Koch and Morgan, 1988). For example, if a set of poorly sampled time intervals is followed by a very well known interval, many species will be first encountered in the better sampled interval even if the true origination occurred in a previous interval.

We acknowledge that our sample of radiolarian diversity within any one stratigraphic bin is incomplete. In the current data set, the maximum richness recovered from a three my interval was 167 species/subspecies. This represents less than 60% of the diversity potentially preserved within a single sample of extremely good preservation (i.e. manganese carbonate nodules, Yao and Baumgartner, 1995). However, an incomplete record is not necessarily inadequate to test hypotheses regarding the history of life over broad stratigraphic and spatial scales (Raup, 1979; Paul, 1998). We have compiled a large number of samples representing a significant proportion of all known distribution data for the Middle Jurassic to Early Cretaceous. In addition, we have applied analytical methods in an attempt to minimize the likelihood of interpreting spurious patterns resulting from biases in preservation, sampling, and uneven taxonomic coverage. The results presented here are broad in scope, and our primary goal is to describe the long-term signal of change in Middle Jurassic to Early Cretaceous radiolarian biota. We hope that the results will help focus future sampling effort on stratigraphic intervals in which radiolarian assemblages are poorly known.

Plots of cumulative curves of sampling effort were produced to assess the proportion of the taxonomic pool which was recovered in each stage (Fig. 5). These curves summarize the number of new taxa added to the dataset with the addition of new samples. Each curve includes only samples which are correlated with each subinterval, and samples are added to the dataset in random order. These plots suggest that for most stages, adding more samples to

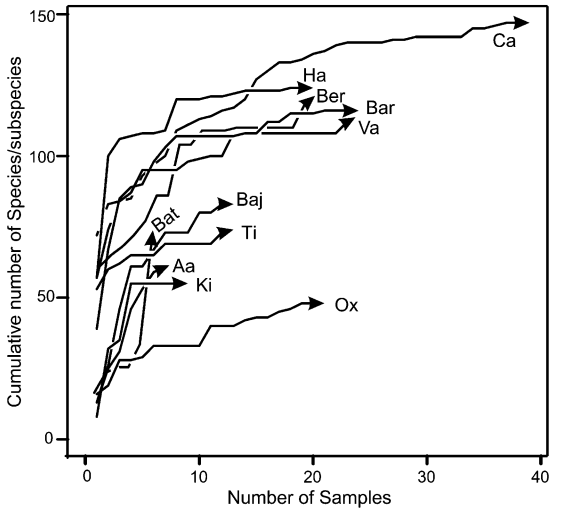

Fig. 5. Plots of cumulative sampling effort for each individual stage. Each line represents the number of unique taxa recorded as samples are added in random order within a single stage. With the addition of more samples, more of the regional species pool is discovered until a theoretical limit is reached beyond which further sampling is unlikely to record new species. This limit is represented in the plot by individual curves reaching a plateau. Chronostratigraphy and stratigraphic stage abbreviations as in Fig. 2.

this dataset will not greatly increase the number of taxa discovered within each stage. However, the cumulative curves also indicate that some stages are not sufficiently sampled (i.e. the Aalenian and Bathonian). Ideally we would fill these gaps with new samples, but instead we determined the effects of the pattern of uneven sampling on the observed pattern of taxic turnover using the stratigraphic permutation test discussed above.

3. The pattern of radiolarian taxic evolution

The Aalenian–Oxfordian is an interval of relatively high first occurrence rates, but few species first occur during the Kimmerdigian–middle Tithonian (Fig. 3b and c). The rate of species first occurrence increased abruptly during the late Tithonian (145–142 Ma), but decreased throughout most of the Early Cretaceous, with the exception of one relatively small peak around the Valanginian/Hauterivian boundary (133–130 Ma). Last occurrence rates varied substantially during the studied interval, but they were overall higher during the Middle and Late Jurassic as compared to the Early Cretaceous. Rates of last occurrence increased during the Oxfordian (157–154 Ma), as well as the middle Bajocian (172–169 Ma) and late Berriasian–early Valanginian (139–136 Ma) to a lesser extent.

The dynamic of evolutionary change is better illustrated by the pattern in the rate of turnover, and even more so, by the rate of diversification (Fig. 3d). The rate of turnover was relatively high during the Aalenian–Oxfordian, but it decreased for the rest of the Late Jurassic, reaching a minimum during the middle Tithonian. Following a late Tithonian pulse, turnover rates were depressed for most of the Early Cretaceous. With the exception of the middle Bajocian, Middle Jurassic diversification rates were positive so that the per taxon rate of species first occurrence was higher than the per taxon rate of species last occurrence. This situation was reversed during the Late Jurassic, when values in diversification rate were negative until the late Tithonian. The Kimmeridgian records the lowest rate of diversification due essentially to a sharp drop in the rate of origination. The trend was again reversed during the early to middle Tithonian as first occurrence rates stabilized but last occurrence rates decreased. The late Tithonian saw the highest diversification rate due to the spectacular pulse in the rate of origination combined with a stabilized extinction rate at low values. With the exception of a gentle late Valanginian–early Hauterivian increase, diversification rates were close to zero for most of the Early Cretaceous. The Barremian–early Aptian deep drop in the rate of diversification is caused by highly accelerated extinction rates and decelerated origination rates. However this decrease in diversification is probably an edge effect.

We analyzed evolutionary rates at the taxonomic level of families to determine whether group membership was controlling evolutionary rate. The plotted age ranges of species within families represented by more than ten species in the database is shown in Fig. 6. The pattern of species first and last occurrence within families does not appear different than the overall pattern of turnover. A permutation test comparing within-family rates of turnover suggested no significant differences among the families.

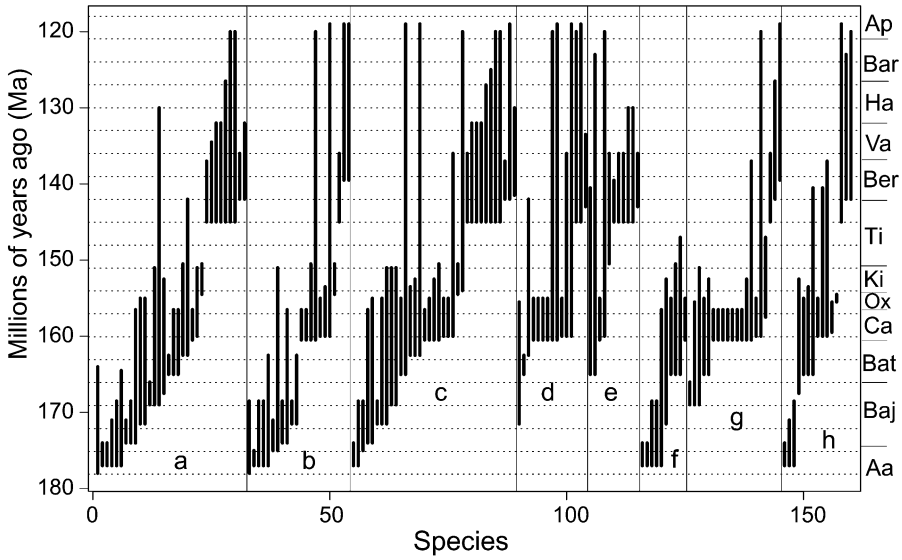

Fig. 6. Stratigraphic ranges of selected radiolarian species/subspecies grouped within families. The following families are included: a = Amphipyndacidae, b = Archaeodictymitridae, c = Parvicingulidae, d = Sethocapsidae, e = Spongocapsulidae, f = Spongodiscidae, g = Theoperidae, h = Tritrabidae. The systematic framework proposed by Dumitrica (1995b) was adopted for this study. Chronostratigraphy and stratigraphic stage abbreviations as in Fig. 2.

Therefore, there is no evidence for taxonomic selectivity in the observed evolutionary pattern.

In order to assess whether the choice of a particular time scale biases the observed pattern, the radiolarian distribution data were reanalyzed using Odin's (1994) time scale (Fig. 7). Some differences can be observed in the Jurassic part of the pattern in the rate of taxic turnover such as the middle Bajocian pulse in the rate of last occurrence. These differences are due to major discrepancies between the selected time scales with respect to the duration of some stages (i.e. the Oxfordian lasts 8 Ma according to Odin (1994), but only 2 Ma according to Pálfy et al. (2000)). It is noteworthy that stage duration but not the absolute age of stage boundaries has a strong influence on the pattern of taxic evolution. This is particularly important because in recent time scales uncertainty in calculating stage duration is much less than uncertainty associated with the calculation of the age of stage boundaries (Gradstein et al., 1995). The pattern in the rate of diversification is in general robust to the choice of time scale. Most of the Middle Jurassic is characterized by positive values, with the exception of a middle Bajocian trough, while values become increasingly negative after the Callovian. The Kimmeridgian records the lowest rate of diversification followed by a spectacular increase close to the Jurassic–Cretaceous boundary.

In order to further assess the extent to which the observed pattern can be influenced by the choice of a particular time scale we examined the pattern in radiolarian faunal changes throughout the various UAZ established by Baumgartner et al. (1995b) (Fig. 8). In this way, faunal changes are observed through time intervals which have various durations, which is the duration of each individual UAZ. The most striking feature of the pattern is the deep trough formed during the late Kimmeridgian–early Tithonian (UAZ 11) and the sharp pulse during the late Tithonian (UAZ 13).

4. Discussion

Following a major extinction event at the end of the Triassic (Carter, 1994), Radiolaria rapidly diversified during the late Hettangian–Sinemurian (Carter et al., 1998), possibly reaching evolutionary equilibrium (sensu Sepkoski, 1978) during the Toarcian–Aalenian with diversity levels of several hundred species (Yao,

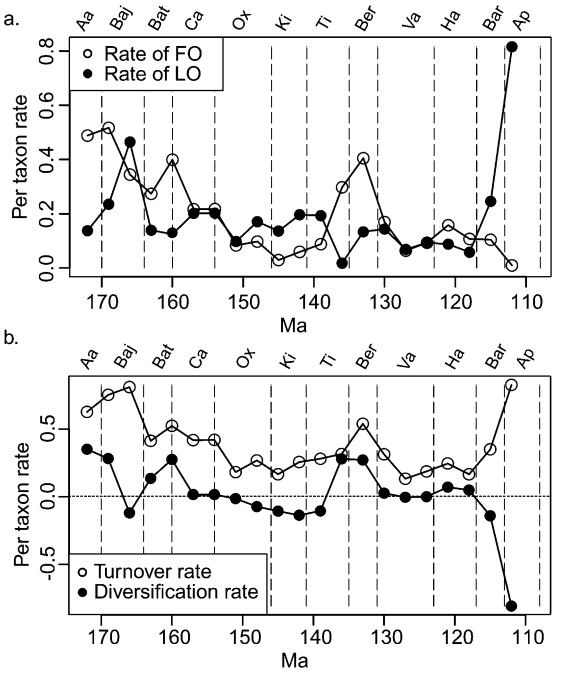

Fig. 7. Plots of the pattern of taxic turnover within the Middle Jurassic to Early Cretaceous radiolaria. In each plot the vertical dashed lines indicate the duration of stratigraphic stages following the timescale of Odin (1994). Each point indicates results for one three-million year subinterval the point being positioned at the end of the subinterval (i.e. the point shown at 169 Ma corresponds to the subinterval 172–169 Ma). (a) Per-taxon rates of first (FO) and last (LO) occurrence. (b) Rates of taxic diversification and turnover. Abbreviations for stratigraphic stages as in Fig. 2.

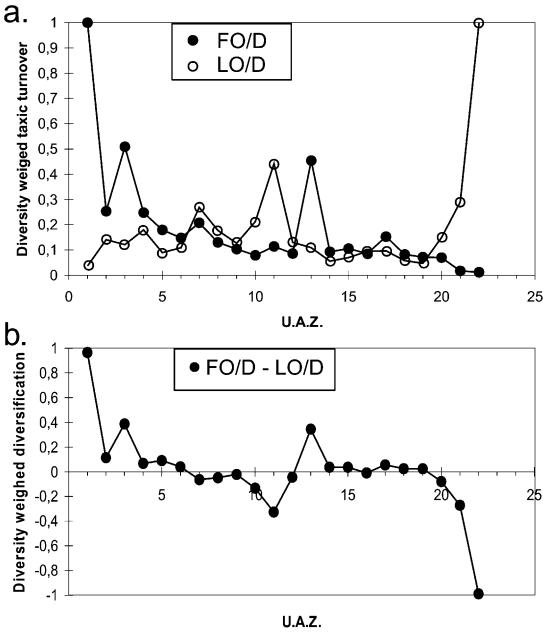

Fig. 8. Plots of the pattern of taxic turnover within the Middle Jurassic to Early Cretaceous radiolarian assemblages analyzed by Baumgartner et al. (1995b). Each point indicates results per Unitary Association Zone (UAZ). (a) Ratio of first (FO) and last (LO) occurrence weighed against sampled diversity (D). (b) Ratio of diversification (FO − LO) weighed against sampled diversity (D).

1997). The importance of subsequent faunal turnovers must be evaluated within the context of the group's evolutionary dynamics.

Two events stand out in the pattern of taxic evolution we obtained from the analysis of Middle Jurassic to Early Cretaceous Tethyan radiolaria. As discussed earlier (Section 3), the rate of diversification appears to be the most reliable amongst the analyzed indices. The index is negative for most of the Late Jurassic, with a lowest value during the Kimmeridgian, followed by a late Tithonian sharp increase. The former is due to last occurrence rates largely surpassing first occurrence rates, as opposed to the late Tithonian, which saw a dramatic pulse of first occurrences combined with a very low rate of last occurrence. It is noteworthy that this pattern is consistent regardless the selected time scale. Also the Kimmeridgian–Tithonian is an interval which appears to be outside any possible sampling bias (see Fig. 4 and Section 2.2).

Both the Kimmeridgian and late Tithonian events coincide with substantial climate derived perturbations in the level of oceanic nutrient availability, suggesting a negative relationship between radiolarian diversity and oceanic productivity. The Carbon isotope curve (Fig. 9) and strong stratigraphic evidence for organic carbon burial and pelagic sedimentary facies, can be used as a proxy to discuss perturbations in the global climate, carbon cycle and overall levels of oceanic nutrient availability. High Late Jurassic nutrient flux to the western Tethyan–Atlantic oceans fuelled overall phytoplankton and radiolarian population growth, resulting in widespread Late Jurassic accumulation of plankton-derived organic matter (Baudin, 1995; Weissert and Mohr, 1996) and radiolarites (Baumgartner, 1987; De Wever et al., 1994). Eutrophication was probably the result of intensified continental weathering under

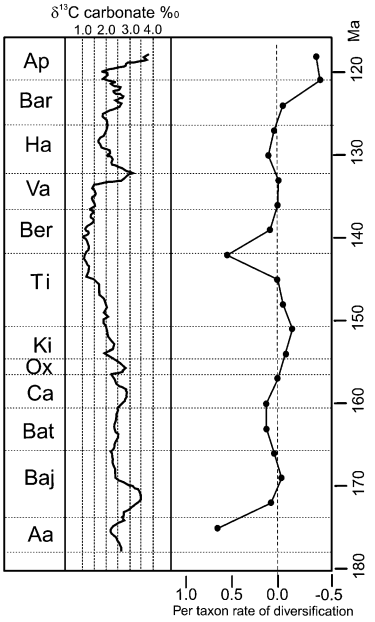

Fig. 9. Middle Jurassic to Early Cretaceous carbon isotope stratigraphy (redrawn after Bartolini et al., 1996; Weissert and Mohr, 1996, and Weissert et al., 1998) against the plot of obtained pattern in the rate of taxic diversification (as in Fig. 3d). Note that points (solid circles) are positioned at the end of each three-million year subinterval. Chronostratigraphy and stratigraphic stage abbreviations as in Fig. 2.

a monsoon-dominated tropical climate (Parrish, 1993; Hallam, 1994; Deconinck et al., 1985) and subsequent increase of nutrient flux from continents to oceans. Various Kimmeridgian/Tithonian palaeoclimatic models suggest that greenhouse conditions were probably the result of intense seafloor spreading, accompanying the ongoing break-up of Pangaea, and associated increase in volcanic CO_2 emissions to the atmosphere (Moore et al., 1992; Valdes and Sellwood, 1992).

Late Jurassic increase in oceanic productivity is first captured by a positive excursion of the $\delta^{13}C$ curve (Fig. 9) and increased organic carbon (C_{org}) burial in a number of basins during the Oxfordian (Weissert and Mohr, 1996). A second pulse of eutrophication occurred during the Kimmeridgian, which led to widespread accumulation of abundant organic matter in epicontinental platforms and margins surrounding western Tethys and central Atlantic (i.e. North Sea, western European and eastern Canadian platforms, Siberia, etc., Baudin, 1995). However, this significant pulse in C_{org} burial is only expressed as a minor excursion of the $\delta^{13}C$ curve. This is because high global sea level favored the growth of Kimmeridgian carbonate platforms and substantially increased the incorporation of carbon in carbonates (C_{cc}), resulting in a stable C_{org}/C_{cc} ratio (Weissert and Mohr, 1996).

A gradual decrease in $\delta^{13}C$ values occurred during the Tithonian. The Kimmeridgian–early Tithonian $\delta^{13}C$ values range near and above +2‰ but drop to values near +1.3‰ in the late Tithonian–early Berriasian. This shift began during the late Tithonian and it coincides with a substantial global sea level fall (Haq et al., 1987; Hallam, 1988) and a reorganization of the global climate system (Weissert and Mohr, 1996). The monsoon-dominated Late Jurassic climate regime acting in the opening Atlantic–western Tethyan oceans and surrounding continents was progressively replaced by a more zonal (and substantially less humid) Early Cretaceous palaeoclimate. The change was accompanied by a shift in the major rainfall zones to equatorial palaeolatitudes. The result was a substantial decrease of terrestrial weathering and transport of nutrients to the oceans. This major climatic change coincides with drastic reduction in the clay flux to the ocean (Hallam, 1994), a drop in $\delta^{13}C$ values (Fig. 9;Weissert and Channell, 1989; Weissert and Mohr, 1996), and the switch of pelagic sedimentary facies in western Tethys from radiolarite to nannoconus-rich Maiolica limestone (Baumgartner, 1987; De Wever et al., 1994). Calcareous nannoconnids were probably dinoflagellates able to bloom in oligotrophic waters (Busson and Noël, 1991). Our results suggest that such long-term changes in nutrient flux to the oceans and associated changes in oceanic productivity had a strong effect on the radiolarian fauna during the relatively warm and permanent-ice-free Jurassic and Cretaceous Periods.

The relationship between diversity and productivity is of much interest to ecologists. A unimodal or hump-shaped pattern seems to exist on a regional scale (i.e. 10^6 km^2). As productivity increases from low to moderate levels diversity tends to increase, but diversity decreases beyond some optimal level of productivity (Rosenzweig and Abramsky, 1993). Determining the role of oceanic nutrient supply in

the evolution of marine biosphere and in particular to mass extinction events in the plankton and benthos is also a major research topic for palaeobiology (e.g. Paul and Mitchell, 1994; Martin 1995, 1996; Murphy et al., 2000). There are currently two different hypotheses regarding the relationship between productivity and diversity based on the fossil record, but neither is fully supported by the available data.

In the energy-bound approach of Vermeij (1995), increasing the supply of raw materials to an environment results in biological diversification. Diversification is a macroevolutionary effect of increased population growth rates and decreased ecological constraint on innovation. Improved resource availability would result in a relaxation of ecological constraint on innovation by reducing the ecological cost of new adaptations. Reduction in resource supply would result in extinction by limiting ecological opportunity.

An alternative model was refined by Hallock (1987) on an initial suggestion by Valentine (1971). The model considers the impact of resource availability within a continuum of trophic resources (CTR) ranging from the oligotrophic subtropical gyres to the highly eutrophic coastal upwelling environments. According to this model, reduction in nutrient supply should encourage organisms to diversify, as more ecological niches and longer and more complex food chains are available in an expanding CTR. On the contrary, increase of nutrient supply would lead to extinctions, because of the expansion of nutrient-rich environments and the resulting contraction of CTR through reduction of oligotrophic niches. The CTR model has a number of points in common with the environmental heterogeneity model discussed by Rosenzweig and Abramsky (1993). Under the environmental heterogeneity model, productivity increase beyond a moderate level can reduce spatial and temporal habitat heterogeneity. For example, annual variation in nutrient supply may decrease. If this happens, diversity declines because the variety of viable temporal specializations is decreased.

The geographical distribution of marine plankton such as radiolaria is in general considered to be dictated by temperature, nutrients and the distribution of oceanic currents that delineate water masses with well-defined barriers. Moreover, recent molecular studies on planktonic foraminifera stress the importance in the differential ecological preference of genetically discriminated species with respect to the productivity levels (as reflected in chlorophyll α concentrations) of the water masses in which they live (de Vargas et al., 1999; see also discussion in Norris and de Vargas, 2000). The ecological niches of extant radiolaria are essentially based on feeding strategy, and four main niches have been identified so far (Casey et al., 1979; Casey, 1993; Anderson, 1983, 1993). These include the near-surface-dwelling symbiont-bearing radiolaria, that meet most of their energy needs from photosynthesis of the endosymbionts, and the bacterivore and nannoherbivore radiolaria, that are abundant near the nutricline at mid latitudes. The fourth group includes the detritivore radiolaria that feed on organic matter. Lazarus (1983) and Lazarus et al. (1995) have presented a strong case for the sympatric and/or depth-parapatric model of speciation as being common in radiolaria (as well as planktonic foraminifera). It is thus possible that radiolarian evolutionary events (i.e. speciation and extinction) were linked to long-term changes (i.e. several 10^5 to several 10^6 years) in nutrient supply and productivity of oceanic water masses.

Our results seem to support Hallock's model and suggest that Kimmeridgian eutrophication of western Tethys favored oligotaxic (low diversity) radiolarian communities. In contrast, it is likely that the late Tithonian substantial decrease in nutrient availability resulted in new ecological opportunities that were rapidly occupied by new radiolarian species. However robust conclusions will require better age resolution than is currently available.

Acknowledgements

T.D. thanks to the Royal Society of Edinburgh (B.P. Grant) for funding his research work in Edinburgh (U.K.). K.G.J. received support from a United Kingdom Natural Environment Research Council Advanced Postdoctoral Fellowship. The authors are grateful to Wolfgang Kiessling, Norman Macleod and particularly Dave Lazarus for constructive remarks during the review process. Claude Abrial assisted with the drawing of some of the figures.

Appendix A

List of samples used in the present analysis. For each sample are given: (a) its number as in the original publication, (b) its chronostratigraphic age as this is inferred by age-diagnostic fossils other than radiolaria or by isotope and magnetostratigraphy, (c) the absolute ages (in my) of both the base and top of its chronostratigraphic age, first according to the time scales of Pálfy et al. (2000, Jurassic) and Gradstein et al. (1995, Cretaceous), secondly after the time scale of Odin (1994), (d) the locality, (e) the lithology, and (f) the reference of the original publication, as follows: '1' Baumgartner and Matsuoka (1995), '2' Bartolini et al. (1995), '3' O'Dogherty et al. (1995), '4' Baumgartner et al. (1995d), '5' Baumgartner (1995), '6' Gorican (1995), '7' Dumitrica (1995a), '8' Danelian (1995), '9' Dumitrica-Jud (1995)

Sample	Relative age	Pálfy–Gradstein		Odin (1994)		Locality	Llthology	Ref.
		Base	Top	Base	Top			
126-4-140	Callovian	−160.5	−156.5	−159	−155	DSDP-534A, Central N. Atlantic	Claystone/shale and calcareous claystone	1
126-2-125	Callovian	−160.15	−156.5	−159	−155	DSDP-534A, Central N. Atlantic	Claystone/shale and calcareous claystone	1
126-2-045	Callovian	−160.5	−156.5	−159	−155	DSDP-534A, Central N. Atlantic	Claystone/shale and calcareous claystone	1
126-2-065	Callovian	−160.5	−156.5	−159	−155	DSDP-534A, Central N. Atlantic	Claystone/shale and calcareous claystone	1
125-6-063	Callovian	−160.5	−156.5	−159	−155	DSDP-534A, Central N. Atlantic	Claystone/shale and calcareous claystone	1
125-6-013	Callovian	−160.5	−156.5	−159	−155	DSDP-534A, Central N. Atlantic	Claystone/shale and calcareous claystone	1
125-5-111	Calloviari	−160.5	−156.5	−159	−155	DSDP-534A, Central N. Atlantic	Claystone/shale and calcareous claystone	1
125-5-072	Callovian	−160.5	−156.5	−159	−155	DSDP-534A, Central N. Atlantic	Claystone/shale and calcareous claystone	1
125-4-001	Callovian	−160.5	−156.5	−159	−155	DSDP-534A, Central N. Atlantic	Claystone/shale and calcareous claystone	1
125-2-115	Callovian	−160.5	−156.5	−159	−155	DSDP-534A, Central N. Atlantic	Claystone/shale and calcareous claystone	1
125-2-035	Callovian	−160.5	−156.5	−159	−155	DSDP-534A, Central N. Atlantic	Claystone/shale and calcareous claystone	1
124-1-052	Callovian	−160.5	−156.5	−159	−155	DSDP-534A, Central N. Atlantic	Carbonate turbidite	1
124-1-041	Callovian	−160.5	−156.5	−159	−155	DSDP-534A, Central N. Atlantic	Claystone/shale and calcareous claystone	1
106-1-029	Kimmeridgian	−154.5	−150.5	−143	−141	DSDP-534A, Central N. Atlantic	Carbonate turbidite	1
089-2-047	Berriasian	−142	−137	−134	−131	DSDP-534A, Central N. Atlantic	Clayey pelagic limestone	1
081-2-064	L.Berriasian–E.Valanginian	−138	−136	−132	−130	DSDP-534A, Central N. Atlantic	Pelagic limestone	1
081-2-003	L.Berriasian–E.Valanginian	−138	−136	−132	−130	DSDP-534A, Central N. Atlantic	Clayey pelagic limestone	1
CB2_45.00	Early Bajocian	−174	−171	−170	−168	CoIle_Bertone, Umbria–Marche, Italy	Pelagic limestone with chert nodules	2
TM_25.15	Middle Aalenian	−177	−175	−174	−171	Terminilletto, Umbria–Marche, Italy	Pelagic limestone with chert nodules	2
TM_29.52	Middle Aalenian	−177	−175	−174	−171	Terminilletto, Umbria–Marche, Italy	Pelagic limestone with thin chert ribbons	2
TM_40.15	Middle Aalenian	−177	−175	−174	−171	Terminilletto, Umbria–Marche, Italy	Pelagic limestone with intercalations of calciturbidite	2
TM_48.35	Middle–Late Aalenian	−177	−174	−173	−170	Terminilletto, Umbria–Marche, Italy	Pelagic limestone with thin chert ribbons	2
TM_51.44	Middle–Late Aalenian	177	−174	−173	−170	Terminilletto, Umbria–Marche, Italy	Pelagic limestone with chert nodules	2
TM_64.74	Late Aalenian	−175	−174	−171	−170	Terminilletto, Umbria–Marche, Italy	Pelagic limestone with intercalations of calciturbidite	2
TM_90.32	Early Bajociara	−174	−171	−170	−168	Terminilletto, Umbria–Marche, Italy	Pelagic limestone with chert nodules	2
TM_105.50	Middle Bajocian	−171.5	−168.5	−168	−166	Terrainilletto, Umbria–Marche, Italy	Pelagic limestone with thin chert ribbons	2
TM_109.25	Middle Bajocian	−171.5	−168.5	−168	−166	Terminilletto, Umbria–Marche, Italy	Pelagic limestone with thin chert ribbons	2
TM_163.05	Middle Bathonian	−165	−162.5	−163	−161.5	Terminilletto, Umbria–Marche, Italy	Pelagic limestone with thin chert ribbons	2
JA4-2	M.– L.Oxfordian (*p.p.*)	−156	−155	−150	−147	Harana, Subbetic, Spain	–	3
89CB-7	Early Bathonian	−166	−164.5	−164	−163	Casa_Blanca, Subbetic, Spain	–	3
89N-M-16	Late Bathonian	−162.5	−160.5	−161.5	−160	Cerro_de_la_Martina, Subbetic, Spain	Marl?	3
CB-7	Early Bathonian	−166	−164.5	−164	−163	Section_58_L0_CB_7	Siliceous limestone with occasional replacement chert	3
POB1784	Late Bajocian	−169	−166	−166	−164	Sierra_de_Ricote, Subbetic, Spain	Siliceous mart	3
POB1785	Late Bajocian	−169	−166	−166	−164	Sierra_de_Ricote, Subbetic, Spain	Siliceous limestone with occasional replacement chert	3
POB1 786	Late Bajocian	−169	−166	−166	−164	Sierra_de_Ricote, Subbetic, Spain	Siliceous limestone with occasional replacement chert	3
POB1 788	Late Bajocian	−169	−166	−166	−164	Sierra_de_Ricote, Subbetic, Spain	Siliceous limestone with occasional replacement chert	3
P0B1789	Late Bajocian	−169	−166	−166	−164	Sierra_de_Ricote, Subbetic, Spain	Siliceous limestone with occasional replacement chert	3
POB1 792	Late Bajocian L.Bajocian–E.Bathonian	−169	166	−166	−164	Sierra_de_Ricote, Subbetic, Spain Sierra_de_Ricote, Subbetic, Spain	Siliceous limestone with occasional replacement chert siliceous limestone	3
POB1796	L.Bajocian–E.Bathonian	−167.5	−164	−165	−164.5	Sierra_de_Ricote, Subbetic, Spain	Siliceous limestone	3
POB1 797	L.Bajocian–E.Bathonian	−167.5	−164	−165	−162.5	Sierra_de_Ricote, Subbetic, Spain	Siliceous limestone	3
P0B1 775	E.Callovian–E.Kimmeridgian	−160.5	−152.5	−160	−144	Sierra_de_Ricote, Subbetic, Spain	Siliceous shale	3

Appendix A (*continued*)

Sample	Relative age	Pálfy–Gradstein		Odin (1994)		Locality	Lithology	Ref.
		Base	Top	Base	Top			
P0B1 730	E.Callovian−E.Kimmeridgian	−160.5	−152.5	−160	−144	Sierra_de_Ricote, Subbetic, Spain	Cherty limestone	3
P0B1 731	E.Callovian−E.Kirmmeridgian	−160.5	−152.5	−160	−144	Sierra_de_Ricote, Subbetic, Spain	Siliceous limestone	3
P0B1 732	E.Callovian–E.Kimmeridgian	−160.5	−152.5	−160	−144	Sierra_de_Ricote, Subbetic, Spain	Siliceous shale	3
POB1 773	E.Callovian–E.Kimmeridgian	−160.5	−152.5	−160	−144	Sierra_de_Ricote, Subbetic, Spain	Siliceous limestone	3
POB1 772	E.Calloviara–E.Kimrneridgian	−160.5	−152.5	−160	−144	Sierra_de_Ricote, Subbetic, Spain	Siliceous limestone	3
POB1 771	E.Callovian–E.Kimmeridgian	−160.5	−152.5	−160	−144	Sierra_de_Ricote, Subbetic, Spain	Siliceous limestone	3
POB1 770	E.Callovian–E.Kimmeridgian	−160.5	−152.5	−160	−144	Sierra_de_Ricote, Subbetic, Spain	Siliceous limestone	3
POB1 746	E.Callovian–E.Kimmeridgian	−160.5	−152.5	−160	−144	Sierra_de_Ricote, Subbetic, Spain	Siliceous shale	3
P0B1 750	E.Callovian–E.Kimmeridgian	−160.5	−152.5	−160	−144	Sierra_de_Ricote, Subbetic, Spain	Siliceous limestone	3
P0B1753	E.Callovian–E.Kimmeridgian	−160.5	−152.5	−160	−144	Sierra_de_Ricote, Subbetic, Spain	Siliceous limestone	3
POB1 776	E.Callovian–E.Kimmeridgian	−160.5	−152.5	−160	−144	Sierra_de_Ricote, Subbetic, Spain	Siliceous limestone	3
POB1 777	E.Callovian–E.Kimmeridgian	−160.5	−152.5	−160	−144	Sierra_de_Ricote, Subbetic, Spain	Siliceous limestone	3
P0B1754	E.Callovian–E.Kimmeridgian	−160.5	−152.5	−160	−144	Sierra_de_Ricote, Subbetic, Spain	Siliceous limestone	3
P0B1778	E.Callovian–E.Kimmeridgian	−160.5	−152.5	−160	−144	Sierra_de_Ricote, Subbetic, Spain	Siliceous shale	3
P0B1779	E.Callovian–E.Kimmeridgian	−160.5	−152.5	−160	−144	Sierra_de_Ricote, Subbetic, Spain	Siliceous shale	3
POB1 755	Early Kimmeridgian	−154.5	−152.5	−146	−144	Sierra_de_Ricote, Subbetic, Spain	Cherty limestone	3
P0B1757	Early Kimmeridgiari	−154.5	−152.5	−146	−144	Sierra_de_Ricote, Subbetic, Spain	Cherty limestone	3
POB1 760	E.Kimm.– E.Tithonian (*p.p.*)	−154	−147	−145	−139	Sierra_de_Ricote, Subbetic, Spain	Limestone	3
P0B1766	E.Kimm.– E.Tithonian (*p.p.*)	−154	−147	−145	−139	Sierra_de_Ricote, Subbetic, Spain	Cherty limestone	3
P0B1768	E.Kimm.– E.Tithonian (*p.p.*)	−154	−147	−145	−139	Sierra_de_Ricote, Subbetic, Spain	Cherty limestone	3
Rl_H_2.70	Early Tithonian	−150.5	−146	−141	−138	Sierra_de_Ricote, Subbetic, Spain	Cherty limestone	3
POB_1695	E.Callovian–M.Oxf. (*p.p.*)	−159.5	−155.5	−158	−150	Ceniga, Trento Plateau, N.ltaly	Siliceous limestone with lenses of chert	4
POB_1704	M.Oxford.– E.Kimm. (pp.)	−155.5	−153.5	−150	−145	Ceniga, Trento Plateau, N.ltaly	Siliceous limestone with lenses of chert	4
POB_1703	M.Oxford.–E.Kimm. (pp.)	−155.5	−153.5	−150	−145	Ceniga, Trento Plateau, N.ltaly	Siliceous limestone with lenses of chert	4
POB_1701	M.Oxford.– E.Kimm. (pp.)	−155.5	−153.5	−150	−145	Ceniga, Trento Plateau, N.ltaly	Siliceous limestone with lenses of chert	4
MCA 0.35	E.Callovian–M.Oxf. (*p.p.*)	−159.5	−155.5	−158	−150	Madona_della_Corona, Trento, N.ltaly	Chert layer intercalated with siliceous limestones	4
MCB_O.9O	Middle Oxfordian	−156	−155	−151.5	−148.5	Madona_della_Corona, Trento, N.ltaly	Chert layer intercalated with siliceous limestones	4
MCB_O.35	Mid.–Late Oxfordian	−155.5	−154.5	−150	−146	Madona della Corona, Trento, N.ltaly	Chert layer intercalated with siliceous limestones	4
K12.00	LCallovian–M.Oxfordian	−157.5	−155	−156	−150	Kaberlaba, Trento Plateau, N.ltaly	Siliceous limestone with lenses of chert	4
13.40	Mid.– Late Oxfordian (*p.p.*)	−156	−155	−151.5	−148.5	Kaberlaba, Trento Plateau, N.ltaly	Siliceous limestone with lenses of chert	4
M18.20	E.Callovian–M.Oxf. (*p.p.*)	−159.5	−155.5	−158	−150	Mazze, Trento Plateau, N.ltaly	Siliceous limestone with lenses and layers of chert	4
M20.60	M.Oxford.– E.Kimm. (*p.p.*)	−155.5	−153.5	−150	−145	Mazze, Trento Plateau, N.ltaly	Siliceous limestone with lenses and layers of chert	4
M21.7'5	M.Oxford.– E.Kimm. (pp.)	−155.5	−153.5	−150	−145	Mazze, Trento Plateau, N.ltaly	Siliceous limestone with lenses and layers of chert	4
POBT34I	Early Bajocian	−174	−171	−170	−168	Sogno, Lombardy Basin, N. Italy	Siliceous limestone with chert nodules	4
Bo230.80	Middle Bajocian	−1715	−168.5	−168	−166	Bosso, Umbria–Marche, Italy	Siliceous limestone with chert nodules	5
V135.50	Earliest Bajocian	−174	−172	−170	−169	Valdorbia, Umbria–Marche, Italy	Siliceous limestone with chert nodules	5
Bed_67-4	Latest Valanginian	−133.5	−132	−124.5	−123	P0B38_VEVEYSE_DE_CH_ST_DENIS	Clayey limestone containing pyritized Radiolaria	5
POB_1 584	Late Kimmeridgian	−152.5	−151	−144	−142	Campo_al_Bello, Umbria Marche, Italy	Marly limestone with chert layers and nodules	5
MN7.30	L.Bajocian–L.Kimmeridgian	−169	−151	−166	−142	Ranch_Superiore, Umbria Marche, Italy	Siliceous limestone with chert nodules	5
MN6.60	L.Bajocian–L.Kimmeridgian	−169	−151	−166	−142	Ranch_Superiore, Umbria Marche, Italy	Siliceous limestone with chert nodules	5
MN3.00	L.Bajocian–L.Kimmeridgian	−169	−151	−166	−142	Ranch_Superiore, Umbria Marche, Italy	Limestone	5
P0B1205	Earliest Berriasian	−142	−140.5	−135	−134	Rusconi-Sangiano, Lombardy Basin, Italy	Chert bed	5
RUO.50	Late Tithoriian	−144.5	−142	−136.5	−135	Rusconi-Sangiano, Lombardy Basin, Italy	Siliceous limestone	5
RK1083	Latest Tithonian	−143.5	−142	−136	−135	Fiume Bosso, Umbria Marche, Italy	Siliceous limestone	5
RK1082	Latest Tithonian	−143.5	−142	−136	−135	Fiume Bosso, Umbria Marche, Italy	Siliceous limestone	5
GL123	E.Aalenian–E.Bajocian	−178	−171	−175	−168	Gornja-Lastva, Budva Trough, Croatia	Ribbon bedded chert	6
PJ_6	E.Callovian–M.Oxfordian	−160	−155	−159	−149	Pojorita, East. Carpathians, Romania	Laminated dolomite	7
PJ_7	E.Callovian–M.Oxfordian	−160	−155	−159	−149	Pojorita, East. Carpathians, Romania	Radiolarite	7
PJ_8	E.Callovian–M.Oxfordian	−160	−155	−159	−149	Pojorita, East. Carpathians, Romania	Radiolarite	7
PJ_9	E.Callovian–M.Oxfordian	−160	−155	−159	−149	Pojorita, East. Carpathians, Romania	Radiolarite	7

Appendix A (*continued*)

Sample	Relative age	Pálfy–Gradstein		Odin (1994)		Locality	Llthology	Ref.
		Base	Top	Base	Top			
PJ_lO	E.Callovian–M.Oxtordiara	−160	−155	−159	−149	Pojorita, East. Carpathians, Romania	Pyrite-bearing radiolarite	7
PJ_l 1	E.Callovian–M.Oxfordian	−160	−155	−1S9	−149	Pojorita, East. Carpathians, Romania	Pyrite-bearing radiolarite	7
PJ_1 2	E.Callovian–M.Oxfordian	−160	−155	−159	−149	Pojorita, East. Carpathians, Romania	Pyrite-bearing radiolarite	7
PJ_13	E.Callovian–M.Oxfordian	−160	−155	−159	−149	Pojorita, East. Carpathians, Romania	Pyrite-bearing radiolarite	7
PJ_14	E.Callovian–M.Oxfordian	−160	−155	−159	−149	Pojorita, East. Carpathians, Romania	Pyrite-bearing radiolarite	7
PJ_15	E.Callovian–M.Oxfordian	−160	−155	−159	−149	Pojorita, East. Carpathians, Romania	Pyrite-bearing radiolarite	7
PJ_16	E.Callovian–M.Oxfordian	−160	−155	−159	−149	Pojorita, East. Carpathians, Romania	Pyrite-bearing radiolarite	7
PJ _17	E.Callovian–M.Oxfordian	−160	−155	−159	−149	Pojorita, East. Carpathians, Romania	Pyrite-bearing radiolarite	7
PJ_1 8	E.Callovian–M.Oxfordian	−160	−155	−159	−149	Pojorita, East. Carpathians, Rômania	Pyrite-bearing radiolarite	7
PJ_1 9	E.Callovian–PviOxfordian	−160	−155	−159	−149	Pojorita, East. Carpathians, Romania	Pyrite-bearing radiolarite	7
PJ_2O	E.Callovian–M.Oxfordian	−160	−155	−159	−149	Pojorita, East. Carpathians, Romania	Pyrite-bearing radiolarite	7
PJ_21	E.Callovlan–M.Oxfordian	−160	−155	−159	−149	Pojorita, East. Carpathians, Romania	Pyrite-bearing radiolarite	7
PJ_22	Ecallovian–M.Oxtordian	−160	−155	−159	149	Pojorita, East. Carpathians, Romania	Radiolarite	7
PJ_23	E.Callovlan–M.Oxfordian	−160	−155	−159	−149	Pojorita, East. Carpathians, Romania	Radiolarite	7
PJ_24	E.Callovian–M.Oxfordian	−160	−155	−159	−149	Pojorita, East. Carpathians, Romania	Radiolarite	7
J_25	E.Callovian–M.Oxfordian	−160	−155	−159	−149	Pojorita, East. Carpathians, Romania	Radiolarite	7
ASB1-6	Early Berriasian	−142	−139.5	−135	−133	Kato Kouklessi, lonian zone, Greece	Chert interbedded with siliceous limestone	8
ASB1-7	Early Berriasian	−142	−139.5	−135	−133	Kato Kouklessi, lonian zone, Greece	Chert interbedded with siliceous limestone	8
V-10.00	Early Berriasian	−142	−139.5	−135	−133.5	Valdorbia, Umbria Marche, Italy	Limestone with chert layer and nodules	9
V-6.50	Late Tithonian	−145	−142	−137	−135	Valdorbia, Umbria Marche, Italy	Limestone with chert layer and nodules	9
V-6.20	Late Tithonian	−145	−142	−137	−135	Valdorbia, Umbria Marche, Italy	Limestone with chert layer and nodules	9
V-6.00	Late Tithonian	−145	−142	−137	−135	Valdorbia, Umbria Marche, Italy	Limestone with chert layer and nodules	9
Bo361.80	Late Berriasian	−139.5	−137.5	−133	−131.5	Fiume Bosso, Umbria Marche, Italy	Siliceous limestone	9
Bo323.20	Early Berriasian (pp.)	−141.5	−140	−134.5	−133.5	Fiume Bosso, Umbria Marche, Italy	Siliceous limestone	9
Bo315.50	Latest Tith.– earliest Berr.	−143	−141	−135.5	−134.5	Fiume Bosso, Umbria Marche, Italy	Siliceous limestone with chert bands or nodules	9
Bo312.90	Latest Tith.–earliest Berr.	−143	−141	−135.5	−134.5	Fiume Bosso, Umbria Marche, Italy	Siliceous limestone with chert bands or nodules	9
Bo312.00	Latest Tith.–earliest Berr.	−143	−141	−135.5	−134.5	Fiume Bosso, Umbria Marche, Italy	Siliceous limestone with chert bands or nodules	9
Bo311.20	Latest Tith.– earliest Berr.	−143	−141	−135.5	−134.5	Fiume Bosso, Umbria Marche, Italy	Siliceous limestone with chert bands or nodules	9
Bo306.20	Late Tithonian	−145	−142	−137	−135	Fiume Bosso, Umbria Marche, Italy	Siliceous limestone with chert bands or nodules	9
Bo305.00	Late Tithonian	−145	−142	−137	−135	Fiume Bosso, Umbria Marche, Italy	Siliceous limestone with chert bands or nodules	9
Bo304.00	Late Tithonian	−145	−142	−137	−135	Fiume Bosso, Umbria Marche, Italy	Siliceous limestone with chert bands or nodules	9
Bo_391.20	Earliest Valanginian	−137	−136	−130.5	−129	Fiume Bosso, Umbria Marche, Italy	Siliceous limestone	9
BO_382.00	Latst Berr.– Earliest Val.	−138	−136.5	−131.5	−130.5	Fiume Bosso, Umbria Marche, Italy	Siliceous limestone with chert bands or nodules	9
BO_370.10	Late Berriasian	−139.5	−137.5	−133	−131.5	Fiume Bosso, Umbria Marche, Italy	Siliceous limestone	9
BO_351.50	Late Berriasian (*p.p.*)	−140	−138.5	−133.5	−132.5	Fiume Bosso, Umbria Marche, Italy	Siliceous limestone	9
BO_336.20	Early Berriasina	−141	−139.5	−134	−133	Fiume Bosso, Umbria Marche, Italy	Siliceous limestone with chert bands or nodules	9
BO_332.70	Early Berriasina	−141	−139.5	−134	−133	Fiume Bosso, Umbria Marche, Italy	Siliceous limestone	9
CA_10.60	Late Hauteriv.– Berremian	−129	−120	−120	−113	Capriolo, Lombardy Basin, N. Italy	Siliceous limestone	9
CA_15.40	Late Hauteriv.–Berremian	−129	−120	−120	−113	Capriolo, Lombardy Basin, N. Italy	Siliceous limestone	9
CA_18.40	Late Hauteriv.–Berremian	−129	−120	−120	−113	Capriolo, Lombardy Basin, N. Italy	Siliceous limestone	9
CA_28.80	Late Hauteriv.– Berremian	−129	−120	−120	−113	Capriolo, Lombardy Basin, N. Italy	Siliceous limestone	9
CA_37.50	Early Hauterivian (*p.p.*)	−131	−130	−121.5	−121	Capriolo, Lombardy Basin, N. Italy	Siliceous limestone with chert bands or nodules	9
CA_44.35	Early Hauterivian (*p.p.*)	−131	−130	−122	−121	Capriolo, Lombardy Basin, N. Italy	Siliceous limestone with chert bands or nodules	9
CA_46.60	Early Hauterivian (*p.p.*)	−131	−130	−122	−121.5	Capriolo, Lombardy Basin, N. Italy	Siliceous limestone with chert bands or nodules	9
CA_57.85	Earliest Hauterivian	−132	−131	−122.5	−122	Capriolo, Lombardy Basin, N. Italy	Siliceous limestone with chert bands or nodules	9
CA_64.30	Latest Val.– Earliest Haut.	−132.5	−131.5	−123.5	−122.5	Capriolo, Lombardy Basin, N. Italy	Siliceous limestone with chert bands or nodules	9
CA_84.90	Late Valanginian (p.p)	−133.5	−132.5	−124.5	−123.5	Capriolo, Lombardy Basin, N. Italy	Siliceous limestone with chert bands or nodules	9
CA_99.75	Late Valanginian (p.p)	−134	−133	−125.8	−125	Capriolo, Lombardy Basin, N. Italy	Siliceous limestone	9
CA_100.00	Late Valanginian (p.p)	−134	−133	−125.8	−125	Capriolo, Lombardy Basin, N. Italy	Siliceous limestone	9
CA_109.60	Late Valanginian (p.p)	−134.5	−133.5	−127	−125.8	Capriolo, Lombardy Basin, N. Italy	Siliceous limestone	9

Appendix A (*continued*)

Sample	Relative age	Pálfy–Gradstein		Odin (1994)		Locality	Llthology	Ref.
		Base	Top	Base	Top			
CA_114.30	Late Valanginian (p.p)	−134.5	−133.5	−127	125.8	Capriolo, Lombardy Basin, N. Italy	Siliceous limestone	9
CA_118.40	Early Valanginian (*p.p.*)	−135.5	−134.5	−128	−127	Capriolo, Lombardy Basin, N. Italy	Siliceous limestone with chert bands or nodules	9
CA_120.10	Early Valanginian (*p.p.*)	−135.5	−134.5	−128	−127	Capriolo, Lombardy Basin, N. Italy	Siliceous limestone with chert bands or nodules	9
CA_129.80	Early Valanginian (*p.p.*)	−136	−135	−129	−128	Capriolo, Lombardy Basin, N. Italy	Siliceous limestone with chert bands or nodules	9
CA_137.60	Early Valanginian (*p.p.*)	−136	−135.5	−129.5	−129	Capriolo, Lombardy Basin, N. Italy	Siliceous limestone with chert bands or nodules	9
CA_139.80	Earliest Valanginian	−136	−135.5	−129.5	−129	Capriolo, Lombardy Basin, N. Italy	Siliceous limestone with chert bands or nodules	9
CA_144.60	Earliest Valanginian	−137	−136	−130.7	−129.5	Capriolo, Lombardy Basin, N. Italy	Siliceous limestone	9
CA 45.60	Earliest Valanginian	−137	−136	−130.7	−129.5	Capriolo, Lombardy Basin, N. Italy	Siliceous limestone	9
CA_146.20	Earliest Valanginian	−137	−136	−130.7	−129.5	Capriolo, Lombardy Basin, N. Italy	Siliceous limestone	9
CA_146.50	Earliest Valanginian	−137	−136	−130.7	−129.5	Capriolo, Lombardy Basin, N. Italy	Siliceous limestone with chert bands or nodules	9
CA_146.60	Earliest Valanginian	−137	−136	−130.7	−129.5	Capriolo, Lombardy Basin, N. Italy	Siliceous limestone with chert bands or nodules	9
CA_154.00	Latest Berriasian	−138	−137	−131.5	−131	Capriolo, Lombardy Basin, N. Italy	Siliceous limestone with chert bands or nodules	9
CA_162.80	Late Berriasian (*p.p.*)	−139	−137.5	−132.5	−131.5	Capriolo, Lombardy Basin, N. Italy	Siliceous limestone	9
CA_163.00	Late Berriasian (*p.p.*)	−139	−137.5	−132.5	−131.5	Capriolo, Lombardy Basin, N. Italy	Siliceous limestone	9
PR_238.80	Middle Barremian	−124	−123	−115.5	−115	Presale, Umbria–Marche, Italy	Limestone with chert nodules	9
PR_225.30	Early Barremian	−126.5	−125	−117	−116	Presale, Umbria–Marche, Italy	Limestone	9
PR_221.05	Early Barremian	−126.5	−125	−117	−116	Presale, Umbria–Marche, Italy	Limestone with chert nodules	9
PR_220.75	Early Barremian	−126.5	−125	−117	−116	Presale, Umbria–Marche, Italy	Limestone with chert nodules	9
PR_211.35	Latest Haut–Earliest Barr.	−127	−125.5	−117.5	−116.5	Presale, Umbria–Marche, Italy	Limestone with chert nodules	
PR_204.30	Latest Hauterivian	−127.5	−126.5	−118	−117	Presale, Umbria–Marche, Italy	Limestone	9
PR_197.30	Late Hauterivian (p-p.)	−129.5	−128.5	−120	−119	Presale, Umbria–Marche, Italy	Limestone	9
PR_187.15	Early Hauterivian (pp.)	−130.5	−129	−121	−120	Presale, Umbria–Marche, Italy	Interbedded siliceous limestone and chert	9
PR_180.10	Early Hauterivian (pp.)	−131.5	−130	−122	−121	Presale, Umbria–Marche, Italy	Limestone	9
GC_893.30	Late Barr. −Earliest Aptian	−123.5	−119	−115	−112.5	Gorgo-a-Cerbara, Umbria–Marche, Italy	Limestone	9
GC_889.30	Late Barr. –Earliest Aptian	−123.5	−119	−115	−112.5	Gorgo-a-Cerbara, Umbria–Marche, Italy	Limestone	9
GC_887.00	Late Barr.-EarliestAptian	−123.5	−119	−115	−112.5	Gorgo-a-Cerbara, Umbria–Marche, Italy	Limestone	9
GC_882.40	Late Barr. –Earliest Aptian	−123.5	−119	−115	−112.5	Gorgo-a-Cerbara, Umbria–Marche, Italy	Limestone	9
GC_874.65	Middle Baremian	−124	−122.5	−115.5	−114.5	Gorgo-a-Cerbara, Umbria–Marche, Italy	Limestone	9
GC_869.80	Early Barremian (*p.p.*)	−124	−123	−115.5	−115	Gorgo-a-Cerbara, Umbna-Marche, Italy	Interbedded siliceous limestone and chert	9
GC_867.20	Early Barremian (pp.)	−124	−123	−115.5	−115	Gorgo-a-Cerbara, Umbria–Marche, Italy	Limestone with chert nodules	9
GC_859.75	Early Barremian (*p.p.*)	−125	−124	−116	−115.5	Gorgo-a-Cerbara, Umbria–Marche, Italy	Limestone	9
GC_846.35	Earliest Barremian	−126.5	−124.5	−117	−116	Gorgo-a-Cerbara, Umbria–Marche, Italy	Limestone	9
GC_840.30	Earliest Barremian	−126.5	−124.5	−117	−116	Gorgo-a-Cerbara, Umbria–Marche, Italy	Interbedded siliceous limestone and chert	9
GC_837.15	Earliest Barremian	−126.5	−124.5	−117	−116	Gorgo-a-Cerbara, Umbria–Marche, Italy	Interbedded siliceous limestone and chert	9
GC_832.10	Earliest Barremian	−126.5	−124.5	−117	−116	Gorgo-a-Cerbara, Umbria–Marche, Italy	Interbedded siliceous limestone and chert	9
GC_821.45	Latest Hauterivian	−127.5	−126.5	−118	117	Gorgo-a-Cerbara,.Umbria–Marche, Italy	Interbedded siliceous limestone and chert	9
GC_819.75	Latest Hauterivian	−127.5	−126.5	−118	−117	Gorgo-a-Cerbara,.Umbria–Marche, Italy	Interbedded siliceous limestone and chert	9
GC_81 7.90	Latest Hauterivian	−127.5	−126.5	−118	−117120	Gorgo-a-Cerbara, Umbria–Marche, Italy	Limestone with chert nodules	9
GC_814.80	Late Hauterivian (pp.)	−128	−127	−118.5	−117.7	Gorgo-a-Cerbara, Umbria–Marche, Italy	Limestone with chert nodules	9
GC_81 2.25	Late Hauterivian (pp.)	−128	−127	−118.5	−117.7	Gorgo-a-Cerbara, Umbria–Marche, Italy	Interbedded siliceous limestone and chert	9
GC_81 7.90	Latest 1-lauterivian	−127.5	−126.5	−118	−117120	Gorgo-a-Cerbara, Umbria–Marche, Italy	Limestone with chert nodules	9
GC_814.80	Late Hauterivian (pp.)	−128	−127	−118.5	−117.7	Gorgo-a-Cerbara, Umbria–Marche, Italy	Limestone with chert nodules	9
GC_812.25	Late Hauterivian (pp.)	−128	−127	−118.5	−117.7	Gorgo-a-Cerbara, Umbria–Marche, Italy	Interbedded siliceous limestone and chert	9
GC_801.20	Late Hautenvian (*p.p.*)	−129.5	−128.5	−120	−119.3	Gorgo-a-Cerbara, Umbria–Marche, Italy	Interbedded siliceous limestone and chert	9
GC_799.00	Late Hauterivian (pp.)	−129.5	−128.5	−120	−119.3	Gorgo-a-Cerbara, Umbria–Marche, Italy	Interbedded siliceous limestone and chert	9
GC_791.70	Early Hauterivian (*p.p.*)	−130.5	−129	−121	−120	Gorgo-a-Cerbara, Umbria–Marche, Italy	Interbedded siliceous limestone and chert	9
GC_786.70	Early Hauterivian (*p.p.*)	−130.7	−129.5	−121.5	−120.5	Gorgo-a-Cerbara, Umbria–Marche, Italy	Interbedded siliceous limestone and chert	9
POB_141.55	Barremian	−126.5	−120	−117	−113	Breggia, Lombardy Basin, Italy	Marl/shale	9
BR_12.40	Late Haut. –Early Barr.	−128.5	−123	−119	−115	Breggia, Lombardy Basin, Italy	Limestone with chert nodules	9
BR_23.00	Late Haut.–Early Barr.	−128.5	−123	−119	−115	Breggia, Lombardy Basin, Italy	Limestone	9

Appendix A (*continued*)

Sample	Relative age	Pálfy–Gradstein		Odin (1994)		Locality	Lithology	Ref.
		Base	Top	Base	Top			
BR_74.80	Late Valang.–Early Haut.	−133.5	−130	−125	−121	Breggia, Lombardy Basin, Italy	Limestone with chert nodules	9
BR_68.40	Late Valang. –Early Haut.	−133.5	−130	−125	−121	Breggia, Lombardy Basin, Italy	Limestone with chert nodules	9
BR_62.80	Late Valanginian	−134.5	−132	−127	−123	Breggia, Lombardy Basin, Italy	Limestone with chert layer	9
BR_54.70	Late Valanginian	−134.5	−132	−127	−123	Breggia, Lombardy Basin, Italy	Limestone with chert layer	9
BR_49.05	Middle Valanginian	−135.5	−133.5	−128	−125	Breggia, Lombardy Basin, Italy	Limestone with chert nodules	9
BR_39.05	Early Valanginian	−137	−134.5	−131	−127	Breggia, Lombardy Basin, Italy	Limestone with chert nodules	9
BR_34.05	Early Valanginian	−137	−135	−131	−128	Breggia, Lombardy Basin, Italy	Limestone with chert layer	9
BR_28.85	Late Berr. –Early Valang.	−138.5	−136	−132	−129	Breggia, Lombardy Basin, Italy	Limestone with chert layer	9
POB1330	Early Berriasian	−142	−139	−134.5	−132.5	Breggia, Lombardy Basin, Italy	Limestone with chert nodules	9
BrO.03	Earliest Berriasian	−142	−140.5	−135	−134	Breggia, Lombardy Basin, Italy	Limestone	9

References

Anderson, O.R., 1983. Radiolaria. Springer, Berlin, 355 pp.

Anderson, O.R., 1993. The trophic role of planktonic foraminifera and radiolaria. Mar. Microbial. Food Webs 7 (1), 31–51.

Bartolini, A., Baumgartner, P.O., Mattioli, E., 1995. Middle and Late Jurassic radiolarian biostratigraphy of the Colle Bertone and Terminilleto sections (Umbria–Marche–Sabina Apennines, Central Italy): an integrated stratigraphical approach. In: Baumgartner, P.O., O'Dogherty, L., Gorican, S., Urquhart, E., Pillevuit, A., De Wever, P. (Eds.), Middle Jurassic to Lower Cretaceous Radiolaria of Tethys: Occurrences, Systematics, Biochronology. Mém. Géol. (Lausanne) 23, 817–832.

Bartolini, A., Baumgartner, P.O., Hunziker, J., 1996. Middle and Late Jurassic carbon stable-isotope stratigraphy and radiolarite sedimentation of the Umbria–Marche Basin (Central Italy). Eclogae Geol. Helv. 89 (2), 811–844.

Baudin, F., 1995. Depositional controls on the Mesozoic source rocks in the Tethys. In: Huc, A.Y. (Ed.), Paleogeography, Paleoclimates and Source Rocks. AAPG Stud. Geol. 40, 191–211.

Baumgartner, P.O., 1984. A Middle Jurassic–Early Cretaceous low-latitude radiolarian zonation based on Unitary Associations and age of Tethyan radiolarites. Eclogae Geol. Helv. 77 (3), 729–837.

Baumgartner, P.O., 1987. Age and genesis of Jurassic Radiolarites. Eclogae Geol. Helv. 96 (3), 601–626.

Baumgartner, P.O., 1995. Towards a Mesozoic radiolarian database — Updates of the work 1984–1990. In: Baumgartner, P.O., O'Dogherty, L., Gorican, S., Urquhart, E., Pillevuit, E., De Wever, P. (Eds.), Middle Jurassic to Lower Cretaceous Radiolaria of Tethys: Occurrences, Systematics, Biochronology. Mém. Géol. (Lausanne) 23, 689–700.

Baumgartner, P.O., Bartolini, A., 1997. Origin and evolution of the genus *Mirifusus* Pessagno (Middle Jurassic to Early Cretaceous). INTERRAD VIII, Abstract vol., p. 17.

Baumgartner, P.O., Matsuoka, A., 1995. New radiolarian data from DSDP Site 534, Blake Bahama Basin, Central Northern Atlantic. In: Baumgartner, P.O., O'Dogherty, L., Gorican, S., Urquhart, E., Pillevuit, A., De Wever, P. (Eds.), Middle Jurassic to Lower Cretaceous Radiolaria of Tethys: Occurrences, Systematics, Biochronology. Mém. Géol. (Lausanne) 23, 709–715.

Baumgartner, P.O., De Wever, P., Kocher, R.N., 1980. Correlation of Tethyan Late Jurassic–Early Cretaceous events. Cah. Micropaléont. 2, 23–85.

Baumgartner, P.O., O'Dogherty, L., Gorican, S., Urquhart, E., Pillevuit, A., De Wever, P. (Eds.), 1995a. Middle Jurassic to Lower Cretaceous Radiolaria of Tethys: Occurrences, Systematics, Biochronology. Mém. Géol. (Lausanne) 23, 1172.

Baumgartner, P.O., Bartolini, A., Carter, E.S., Conti, M., Cortese, G., Danelian, T., De Wever, P., Dumitrica, P., Dumitrica-Jud, R., Gorican, S., Guex, J., Kito, N., Marcucci, M., Matsuoka, A., Murchey, B., O'Dogherty, L., Savary, J., Vishnevskaya, V., Widz, D., Yao, A., 1995b. Middle Jurassic to Early Cretaceous Radiolarian Biochronology of Tethys based on Unitary Associations. In: Baumgartner, P.O., O'Dogherty, L., Gorican, S., Urquhart, E., Pillevuit, A., De Wever, P. (Eds.), Middle Jurassic to

Lower Cretaceous Radiolaria of Tethys: Occurrences, Systematics, Biochronology. Mém. Géol. (Lausanne) 23, 1013–1043.

Baumgartner, P.O., O'Dogherty, L., Gorican, S., Dumitrica-Jud, R., Dumitrica, P., Pillevuit, A., Urquhart, E., Matsuoka, A., Danelian, T., Bartolini, A., Carter, E.S., De Wever, P., Kito, N., Marcucci, M., Steiger, T., 1995c. Radiolarian catalogue and systematics of Middle Jurassic to Early Cretaceous Tethyan genera and species. In: Baumgartner, P.O., O'Dogherty, L., Gorican, S., Urquhart, E., Pillevuit, A., De Wever, P. (Eds.), Middle Jurassic to Lower Cretaceous Radiolaria of Tethys: Occurrences, Systematics, Biochronology. Mém. Géol. (Lausanne) 23, 37–685.

Baumgartner, P.O., Martire, L., Gorican, S., O'Dogherty, L., Erba, E., Pillevuit, A., 1995d. New Middle and Upper Jurassic radiolarian assemblages co-occuring with ammonites and nannofossils from the Southern Alps (Northern Italy). In: Baumgartner, P.O., O'Dogherty, L., Gorican, S., Urquhart, E., Pillevuit, A., De Wever, P. (Eds.), Middle Jurassic to Lower Cretaceous Radiolaria of Tethys: Occurrences, Systematics, Biochronology. Mém. Géol. (Lausanne) 23, 737–750.

Blome, C.D., Reed, K.M., 1993. Acid processing of pre-Tertiary radiolarian cherts and its impact on fauna content and biozonal correlation. Geology 21, 177–180.

Budd, A.F., Johnson, K.G., 1999. Origination preceding extinction during Late Cenozoic turnover of Caribbean reefs. Paleobiology 25, 188–200.

Budd, A.F., Johnson, K.G., 2001. Contrasting patterns in rare and abundant species during evolutionary turnover. In: Jackson, J.B.C., Lidgard, S., McKinney, F.K. (Eds.), Process From Pattern in the Fossil Record. University Chicago Press, Chicago, in press.

Budd, A.F., Johnson, K.G., Stemann, T.A., 1996. Plio-Pleistocene turnover in the Caribbean reef coral fauna. In: Jackson, J.B.C., Coates, A.G., Budd, A.F. (Eds.), Evolution and Environment in Tropical America. University Chicago Press, Chicago, pp. 168–204.

Busson, G., Noël, D., 1991. Les nannoconidés, indicateurs environnementaux des océans et mers épicontinentales du Jurassique terminal et du Crétacé inférieur. Oceanol. Acta 14 (4), 333–356.

Carter, E.S., 1994. Evolutionary trends in latest Triassic (upper Norian) and earliest Jurassic (Hettangian) Radiolaria. In: Cariou, E., Hantzperque, P. (Eds.), Third International Symposium on Jurassic Stratigraphy, Poitiers 1991, Géobios. Mém. Spéc. 17, 111–119.

Carter, E.S., 1995. Middle Jurassic (Aalenian and early Bajocian) radiolarians from the Queen Charlotte Islands, British Columbia, Canada. In: Baumgartner, P.O., O'Dogherty, L., Gorican, S., Urquhart, E., Pillevuit, A., De Wever, P. (Eds.), Middle Jurassic to Lower Cretaceous Radiolaria of Tethys: Occurrences, Systematics, Biochronology. Mém. Géol. (Lausanne) 23, 977–983.

Carter, E.S., Whalen, P.A., Guex, J., 1998. Biochronology and paleontology of Lower Jurassic (Hettangian and Sinemurian) Radiolarians, Queen Charlotte Islands, British Columbia. Geol. Surv. Can. Bull. 496, 1–162.

Casey, R.E., 1993. Radiolaria. In: Lipps, J.E. (Ed.), Fossil Prokaryotes and Protists. Blackwell, Boston, pp. 249–284.

Casey, R.E., Gust, L., Leavesley, A., Williams, D., Reynolds, R., Duis, T., Spaw, J.M., 1979. Ecological niches of radiolarians, planktonic foraminiferans and pteropods inferred from studies on living forms in the Gulf of Mexico and adjacent waters. Trans. Gulf Coast Assoc. Geol. Soc. 29, 216–223.

Danelian, T., 1995. Middle to Upper Jurassic radiolarian biostratigraphy of the Ionian and Maliac zones (Greece). In: Baumgartner, P.O., O'Dogherty, L., Gorican, S., Urquhart, E., Pillevuit, A., De Wever, P. (Eds.), Middle Jurassic to Lower Cretaceous Radiolaria of Tethys: Occurrences, Systematics, Biochronology. Mém. Géol. (Lausanne) 23, 865–876.

Deconinck, J.F., Beaudoin, B., Joseph, P., Raoult, J.F., 1985. Contrôles tectonique, eustatique, et climatique de la sédimentation argileuse du domaine subalpin français au Malm-Crétacé. Rév. Géol. Dyn. Géogr. Phys. 26, 311–320.

De Wever, P., Azéma, J., Fourcade, E., 1994. Radiolaires et Radiolarites: production primaire, diagenèse et paléogéographie. Bull. Centres Rech. Explor. -Prod. Elf Aquitaine 18 (1), 315–379.

Donovan, S.K., Paul, C.R.C. (Eds.), 1998. The Adequacy of the Fossil Record. Wiley, New York, 312 pp.

Dumitrica, P., 1995a. Biostratigraphy of the Radiolarites at Pojorita (Rarau Syncline, East Carpathians). In: Baumgartner, P.O., O'Dogherty, L., Gorican, S., Urquhart, E., Pillevuit, A., De Wever, P. (Eds.), Middle Jurassic to Lower Cretaceous Radiolaria of Tethys: Occurrences, Systematics, Biochronology. Mém. Géol. (Lausanne) 23, 907–914.

Dumitrica, P., 1995b. Systematic framework of Jurassic and Cretaceous Radiolaria). In: Baumgartner, P.O., O'Dogherty, L., Gorican, S., Urquhart, E., Pillevuit, A., De Wever, P. (Eds.), Middle Jurassic to Lower Cretaceous Radiolaria of Tethys: Occurrences, Systematics, Biochronology. Mém. Géol. (Lausanne) 23, 19–35.

Dumitrica, P., Dumitrica-Jud, R., 1995. Aurisaturnalis carinatus (Foreman), an example of phyletic gradualism among Saturnalid-type radiolarians. Rev. Micropal. 38 (3), 195–216.

Dumitrica-Jud, R., 1995. Early Cretaceous Radiolarian biostratigraphy of Umbria–Marche Apennines (Italy), Southern Alps (Italy and Switzerland) and Hawasina Nappes (Oman). In: Baumgartner, P.O., O'Dogherty, L., Gorican, S., Urquhart, E., Pillevuit, A., De Wever, P. (Eds.), Middle Jurassic to Lower Cretaceous Radiolaria of Tethys: Occurrences, Systematics, Biochronology. Mém. Géol. (Lausanne) 23, 751–797.

Erbacher, J., Thurow, J., 1997. Influence of oceanic anoxic events on the evolution of mid-Cretaceous radiolaria in the North Atlantic and western Tethys. Mar. Micropal. 30, 139–158.

Foote, M., 1994. Temporal variation in extinction risk and temporal scaling of extinction metrics. Paleobiology 20, 424–444.

Foote, M., 2000. Origination and extinction components of taxonomic diversity: Paleozoic and post-Paleozoic dynamics. Paleobiology 26, 578–605.

Foote, M., Raup, D.M., 1996. Fossil preservation and the stratigraphic ranges of taxa. Paleobiology 22, 121–140.

Foreman, H.P., 1973. Radiolaria from Deep Sea Drilling Project Leg 20. Init. Rep. DSDP, XX, 249–305.

Gorican, S., 1995. Middle Jurassic to Early Cretaceous radiolarian biochronology of the Budva Zone (Dinarides, Montenegro). In:

Baumgartner, P.O., O'Dogherty, L., Gorican, S., Urquhart, E., Pillevuit, A., De Wever, P. (Eds.), Middle Jurassic to Lower Cretaceous Radiolaria of Tethys: Occurrences, Systematics, Biochronology. Mém. Géol. (Lausanne) 23, 847–863.

Gradstein, F.M., Agterberg, F.P., Ogg, J.G., Hardenbol, J., van Veen, P., Thierry, J., Huang, Z., 1995. A Triassic, Jurassic and Cretaceous time scale. In: Berggren, W.A., Kent, D.V., Aubry, M.-P., Hardenbol, J. (Eds.), Geochronology, Time Scales and Global Stratigraphic Correlation. SEPM Spec. Publ. 54, 95–126.

Guex, J., 1991. Biochronological Correlations. Springer, Berlin, 250 pp.

Hallam, A., 1988. A re-evaluation of Jurassic eustasy in the light of new data and the revised Exxon curve. In: Wilgus, C.K., Hastings, B.S., Kendall, C.G.St.C., Posamentier, H.W., Ross, C.A., Van Wagoner, J. (Eds.), Sea-Level Changes — an Integrated Approach. SEPM Spec. Publ. 42, 261–273.

Hallam, A., 1994. Jurassic climates as inferred from the sedimentary and fossil record. In: Allen, J.R.L., Hoskins, B.J., Sellwood, B.W., Spicer, R.A., Valdes, P.J. (Eds.), Palaeoclimates and their Modelling. Chapman & Hall, London, pp. 79–88.

Hallock, P., 1987. Fluctuations in the trophic resource continuum: a factor in global diversity cycles? Paleoceanography 2 (5), 457–471.

Haq, B.U., Hardenbol, J., Vail, P.R., 1987. Chronology of fluctuating sea levels since the Triassic. Science 235, 1156–1167.

Hoffman, A., Kitchell, J.A., 1984. Evolution in a pelagic planktic system: a paleobiologic test of models of multispecies evolution. Paleobiology 10 (1), 9–33.

Hollis, C.J., 1996. Radiolarian faunal change through the Cretaceous–Tertiary transition of Eastern Marlborough, New Zealand. In: MacLeod, N., Keller, G. (Eds.), Cretaceous–Tertiary Mass Extinctions: Biotic and Environmental Changes. Norton, New York, pp. 173–204.

Hori, R.S., 1997. The Toarcian radiolarian event in bedded cherts from southwestern Japan. Mar. Micropal. 30, 159–169.

Hull, D.M., 1995. Morphologic diversity and paleogeographic significance of the Family Parvicingulidae (Radiolaria). Micropaleontology 41 (1), 1–48.

Jackson, J.B.C., Johnson, K.G., 2000. Life in the last few million years. In: Erwin, D.H., Wing, S.L. (Eds.), Deep Time: Paleobiology's Perspective. Paleobiology 26 (suppl.), 221–235.

Johnson, K.G., Curry, G.B., 2001. Regional biotic turnover dynamics in the Plio-Pleistocene molluscan fauna of New Zealand. Palaeogeogr. Palaeoclimatol. Palaeoecol. 172, 39–51.

Johnson, K.G., McCormick, T., 1999. The quantitative description of biotic change using palaeontological databases. In: Harper, D. (Ed.), Numerical Palaeobiology. Wiley, New York, pp. 227–247.

Johnson, K.G., Budd, A.F., Stemann, T.A., 1995. Extinction selectivity and ecology of Neogene Caribbean corals. Paleobiology 21, 52–73.

Jud, R., 1994. Biochronology and Systematics of Early Cretaceous Radiolaria of the Western Tethys. Mém. Géol. (Lausanne) 19, 147 pp., 24 pls.

Koch, C.F., 1987. Prediction of sample size effects on the measured teproal and geographic distribution patterns of species. Paleobiology 13, 100–107.

Koch, C.F., Morgan, J.P., 1988. On the expected distribution of species ranges. Paleobiology 14, 126–138.

Lambert, E., De Wever, P., 1996. Événements biologiques chez les radiolaires au cours des phases kénoxiques du Crétacé. Rev. Micropal. 39 (4), 283–292.

Lazarus, D., 1983. Speciation in pelagic protista and its study in the planktonic microfossil record: a review. Paleobiology 9, 327–340.

Lazarus, D., 1998. Book Review of Cretaceous–Paleocene Radiolaria from Eastern Marlborough New Zealand by C.J. Hollis. Mar. Micropal. 34, 245–247.

Lazarus, D., Hilbrecht, H., Spencer-Cervato, C., Thierstein, H., 1995. Sympatric speciation and phyletic change in Globorotalia truncatulinoides. Paleobiology 21 (1), 28–51.

Lisitzin, A.P., 1985. The Silica cycle during the last Ice Age. Palaeogeogr. Palaeoclimatol. Palaeoecol. 50, 241–270.

Marshall, C.R., 1990. Confidence intervals on stratigraphic ranges. Paleobiology 16, 1–10.

Marshall, C.R., 1994. Confidence intervals on stratigraphic ranges: partial relaxation of the assumption of randomly distributed fossil horizons. Paleobiology 20, 459–469.

Martin, R.E., 1995. Cyclic and secular variation in microfossil biomineralization: clues to the biogeochemical evolution of Phanerozoic oceans. Global Planet. Change 11, 1–23.

Martin, R.E., 1996. Secular increase in nutrient levels through the Phanerozoic: implications for productivity, biomass, and diversity of the marine biosphere. Palaios 11, 209–219.

Matsuoka, A., 1983. Middle and Late Jurassic Radiolarian biostratigraphy in the Sakawa and adjacent areas, Shikoku, soutwest Japan. J. Geosci. Osaka Cy Univ. 26 (1), 1–48.

Matsuoka, A., 1995. Middle Jurassic to Early Cretaceous radiolarian occurrences in Japan and the Western Pacific (ODP Sites 800–801). In: Baumgartner, P.O., O'Dogherty, L., Gorican, S., Urquhart, E., Pillevuit, A., De Wever, P. (Eds.), Middle Jurassic to Lower Cretaceous Radiolaria of Tethys: Occurrences, Systematics, Biochronology. Mém. Géol. (Lausanne) 23, 937–966.

Mekik, F.A., 2000. Early Cretaceous Pantanelliidae (Radiolaria) from Northwest Turkey. Micropaleontology 46 (1), 1–30.

Moore, G.T., Hayashida, D.N., Ross, C.A., Jacobson, S.R., 1992. Paleoclimate of the Kimmeridgian/Tithonian (Late Jurassic) world: Results using a general circulation model. Palaeogeogr. Palaeoclimatol. Palaeoecol. 93, 47–72.

Murphy, A.E., Sageman, B.B., Hollander, D.J., 2000. Eutophication by decoupling of the marine biogeochemical cycles of C, N, and P: A mechanism for the Late Devonian mass extinction. Geology 28, 427–430.

Norris, R.D., 2000. Pelagic species diversity, biogeography, and evolution. In: Erwin, D.H., Wing, S.L. (Eds.), Deep Time: Paleobiology's Perspective. Paleobiology 26 (suppl.), 236–258.

Norris, R.D., de Vargas, C., 2000. Evolution at all sea. Nature 405, 23–24.

Odin, G.S., 1994. Geological Time Scale. C. R. Acad. Sci. 318 (II), 59–71.

O'Dogherty, L., 1994. Biochronology and paleontology of Mid-Cretaceous Radiolarians from Northern Apennines (Italy) and Betic Cordillera (Spain). Mém. Géol. (Lausanne) 21, 413 pp., 74 pls.

O'Dogherty, L., Baumgartner, P.O., Sandoval, J., Martin-Algarra, A., Pillevuit, A., 1995. Middle and Upper Jurassic radiolarian assemblages co-occuring with ammonites from the Subbetic Realm (Southern Spain). In: Baumgartner, P.O., O'Dogherty, L., Gorican, S., Urquhart, E., Pillevuit, A., De Wever, P. (Eds.), Middle Jurassic to Lower Cretaceous Radiolaria of Tethys: Occurrences, Systematics, Biochronology. Mém. Géol. (Lausanne) 23, 717–724.

Pálfy, J., Smith, P.L., Mortensen, J.K., 2000. A U–Pb and 40Ar/39Ar time scale for the Jurassic. Can. J. Earth Sci. 37, 923–944.

Parrish, J.T., 1993. Climate of the supercontinent Pangea. J. Geol. 101, 215–233.

Paul, C.R.C., 1982. The adequacy of the fossil record. In: Joysey, K.A., Friday, A. (Eds.), Problems of Phylogenetic Reconstruction. Systematics Assoc. Spec. 2, 75–117.

Paul, C.R.C., 1998. Adequacy, completeness and the fossil record. In: Donovan, S.K., Paul, C.R.C. (Eds.), The Adequacy of the Fossil Record. Wiley, New York, pp. 1–22.

Paul, C.R.C., Mitchell, S.F., 1994. Is famine a common factor in marine mass extinctions? Geology 22, 679–682.

Pessango Jr., E.A., Blome, C.D., 1980. Upper Triassic and Jurassic Pantanelliinae from California, Oregon and British Columbia. Micropaleontology 26 (3), 225–273.

Racki, G., 1999. Silica-secreting biota and mass extinctions: survival patterns and processes. Palaeogeogr. Palaeoclimatol. Palaeoecol. 154, 107–132.

Racki, G., Cordey, F., 2000. Radiolarian palaeoecology and radiolarites: is the present the key to the past? Earth Sci. Rev. 52, 83–120.

Raup, D.M., 1976. Species diversity in the Phanerozoic: an interpretation. Paleobiology 2, 289–297.

Raup, D.M., 1979. Biases in the fossil record of species and genera. Carnegie Mus. Nat. Hist. Bull. 13, 85–91.

Renz, G.W., 1976. The distribution and ecology of radiolaria in the Central Pacific: plankton and surface sediments. Bull. Scripps Inst. Oceanogr. 22, 267.

Roth, P.H., 1987. Mesozoic calcareous nannofossil evolution: relation to paleoceanographic events. Paleoceanography 2 (6), 601–611.

Rosenzweig, M.L., Abramsky, Z., 1993. How are diversity and productivity related? In: Ricklefs, R.E., Schluter, D. (Eds.), Species diversity in ecological communities. Chicago University Press, Chicago, pp. 52–65.

Sepkoski Jr., J.J., 1978. A kinetic model of Phanerozoic taxonomic diversity. I. Analysis of marine orders. Paleobiology 4 (3), 223–251.

Sepkoski Jr., J.J., 1982. A compendium of fossil marine familes. Milwaukee Publ. Mus. Contr. Biol. Geol. 51, 1–125.

Signor III, P.W., 1978. Species richness in the Phanerozoic: an investigation of sampling effects. Paleobiology 4, 394–406.

Signor III, P.W., Lipps, J.H., 1982. Sampling bias, gradual extinction patterns and catastrophes in the fossil record. Geol. Soc. Am. Spec. Pap. 190, 291–296.

Simpson, G.G., 1953. The Major Features of Evolution. Columbia University Press, New York, 413 pp.

Thierry, J., et al. (41 co-authors), 2000. Early Tithonian. In: Dercourt, J., Gaetani, M., et al. (Eds.), Atlas Peritethys, Palaeogeographical maps. CCGM/CGMW, Pars: map 11.

Valdes, P.J., Sellwood, B.W., 1992. A paleoclimate model for the Kimmeridgian. Palaeogeogr. Palaeoclimatol. Palaeoecol. 47, 195–223.

Valentine, J.W., 1971. Ressource supply and species diversity patterns. Lethaia 4, 51–61.

de Vargas, C., Norris, R., Zaninetti, L., Gibb, S.W., Pawlowski, J., 1999. Molecular evidence of cryptic speciation in planktonic foraminifers and their relation to oceanic provinces. Proc. Natl. Acad. Sci. USA 96, 2864–2868.

Vermeij, G.J., 1995. Economics, volcanoes, and Phanerozoic revolutions. Paleobiology 21 (2), 125–152.

Vishnevskaya, V., 1997. Development of Palaeozoic–Mesozoic Radiolaria in Northwestern Pacific Rim. Mar. Micropal. 30, 79–95.

Wei, K.-Y., Kennett, J.P., 1986. Taxonomic evolution of Neogene planktonic Foraminifera and paleoceanographic relations. Paleoceanography 1 (1), 67–84.

Weissert, H., Channell, J.E.T., 1989. Tethyan carbonate carbon isotope stratigraphy across the Jurassic–Cretaceous boundary: an indicator of decelerated global carbon cycling? Paleoceanography 4 (4), 483–494.

Weissert, H., Mohr, H., 1996. Late Jurassic climate and its impact on carbon cycling. Palaeogeogr. Palaeoclimatol. Palaeoecol. 122, 27–43.

Yao, A., 1997. Faunal change of Early–Middle Jurassic radiolarians. News Osaka Micropal. Spec. 10, 155–182.

Yao, A., Baumgartner, P.O., 1995. Radiolarian Occurrence Data from the Middle Jurassic Manganese Carbonates of the Inuyama and Kamiaso Areas, Japan. In: Baumgartner, P.O., O'Dogherty, L., Gorican, S., Urquhart, E., Pillevuit, A., De Wever, P. (Eds.), Middle Jurassic to Lower Cretaceous Radiolaria of Tethys: Occurrences, Systematics, Biochronology. Mém. Géol. (Lausanne) 23, 967–976.

Yao, A., Kuwahara, K., 1997. Radiolarian faunal change from Late Permian to Middle Triassic times. News Osaka Micropal. Spec. 10, 87–96.